



Technical Report HCSU-064

BEHAVIOR OF THE HAWAIIAN HOARY BAT (*LASIURUS
CINEREUS SEMOTUS*) AT WIND
TURBINES AND ITS DISTRIBUTION ACROSS THE NORTH
KO`OLAU MOUNTAINS, O`AHU

P. Marcos Gorresen¹, Paul M. Cryan², Manuela M. Huso³, Cris D. Hein⁴, Michael R. Schirmacher⁴, Jessica A. Johnson¹, Kristina M. Montoya-Aiona⁵, Kevin W. Brinck¹, and Frank J. Bonaccorso⁵

¹Hawai'i Cooperative Studies Unit, University of Hawai'i at Hilo, P.O. Box 44, Hawai'i National Park, HI 96718

²U.S. Geological Survey, Fort Collins Science Center, 2150 Centre Ave., Bldg. C, Fort Collins, CO 80526

³U.S. Geological Survey, USGS Forest and Rangeland Ecosystem Science Center, Forest Sciences Lab, RM 156, 3200 SW Jefferson Way, Corvallis, OR 97331

⁴Bat Conservation International, P.O. Box 162603, Austin, TX 78716

⁵U.S. Geological Survey, Pacific Island Ecosystems Research Center, Kilauea Field Station, P.O.Box 44, Hawai'i National Park, HI 89718

Hawai'i Cooperative Studies Unit
University of Hawai'i at Hilo
200 W. Kawili St.
Hilo, HI 96720
(808) 933-0706

May 2015



UNIVERSITY
of HAWAII[®]
HILO

This product was prepared under Cooperative Agreement CA G12AC20054 for the Pacific Island Ecosystems Research Center of the U.S. Geological Survey.

This article has been peer reviewed and approved for publication consistent with USGS Fundamental Science Practices (<http://pubs.usgs.gov/circ/1367/>). Any use of trade, firm, or product names is for descriptive purposes only and does not imply endorsement by the U.S. Government.

TABLE OF CONTENTS

List of Tables	iv
List of Figures	iv
Abstract.....	1
Introduction.....	1
Methods	2
Study area.....	2
Acoustic sampling and review	4
Recording and review of video imagery	4
Habitat and weather data	6
Bat fatality monitoring.....	7
Fatality searches	7
Field bias trials	8
Data analyses	8
Occupancy analysis of bat distribution	8
Bat behavior at turbines.....	10
Bat fatality monitoring	11
Results	12
Occupancy analysis of bat distribution.....	12
Bat behavior at turbines	18
Bat fatality monitoring.....	35
Bias trials.....	35
Fatality searches	36
Fatality estimation.	37
Discussion	38
Summary of key study findings.....	45
Management implications	46
Acknowledgements	47
Literature Cited	48
Appendix 1. MATLAB code used for finding bats and other targets in thermal surveillance camera footage.....	54
Appendix 2. Occupancy model covariate statistics	64
Appendix 3. Preliminary single-covariate occupancy models.....	65
Appendix 4. Final occupancy models	66
Appendix 5. Fatality model parameters.....	68

LIST OF TABLES

Table 1. Habitat visibility classes of carcass search plots.....	8
Table 2. Model-averaged coefficient estimates for the set of 12 final occupancy models	15
Table 3. Searcher efficiency and carcass persistence models.....	36
Table 4. Top performing models of searcher efficiency and carcass persistence bias trials	36
Table 5. Probability that the total fatalities exceed a specific number of carcasses given the observed count	37

LIST OF FIGURES

Figure 1. Acoustic and video sample sites on north O'ahu, Hawai'i.	3
Figure 2. Video camera field-of-view.	5
Figure 3. Observed nightly bat detection probability by month among survey sites.....	13
Figure 4. Observed nightly bat detection probability by survey site.....	14
Figure 5. Occupancy as a function of time of year and mean nightly temperature	15
Figure 6. Occupancy as a function of time of year and barometric pressure	16
Figure 7. Occupancy a function of time of year and mean nightly relative humidity	16
Figure 8. Occupancy as a function of time of year and wind direction.....	16
Figure 9. Probability of detecting bats as a function of elevation and wind exposure	17
Figure 10. Probability of detecting bats as a function of topographic position and terrain roughness.....	18
Figure 11. Probability of detecting bats as a function of canopy cover and landcover heterogeneity	18
Figure 12. Proportion of video detections of bats by time of night	19
Figure 13. Video detections of bats by time of night over the 6-month monitoring period	20
Figure 14. Video detections of bats per hour by night over the 6-month monitoring period	20
Figure 15. Example of a bat detection from a thermal video image sequence.....	21
Figure 16. Frequency of the duration of video detections of bats.....	22
Figure 17. Mean duration of video detections of bats.....	22
Figure 18. Correspondence between the rate of bat detections and mean nightly wind speed and temperature	24
Figure 19. Cumulative distribution functions of mean wind speed during video detections	25
Figure 20. Cumulative distribution functions of mean temperature during video detections	26
Figure 21. Cumulative distribution functions of barometric pressure during video detections ...	26
Figure 23. Cumulative distribution functions of barometric pressure trend during video detection	28

Figure 24. Cumulative distribution functions of barometric pressure trend over a 24-hour lag period during bat detections	29
Figure 25. Cumulative distribution functions of maximum wind speed during detections of bats	29
Figure 26. Cumulative distribution functions of moon illumination during detections of bats	30
Figure 27. Classification tree model of interactions between weather variables associated with the proportion of bat detections observed by video	31
Figure 28. Regression tree model of interactions between weather variables associated with the rate of bat detections	32
Figure 29. Nightly video detections of bats relative to insect detections	33
Figure 30. Video detections of bats relative to insect detections across all nights	33
Figure 31. Frequency of acoustic detections on nacelle-mounted bat detectors relative to video detections from ground-based surveillance cameras	34
Figure 32. Proportion of acoustic bat detections relative to the hypothetical sampling coverage and overlap of a pair of detector microphones	35
Figure 33. Posterior probability distribution that total fatalities are equal to or exceed a specific number given the total observed carcass count.....	37

ABSTRACT

We studied the landscape distribution of endemic Hawaiian hoary bats (*Lasiurus cinereus semotus*) on the north Ko'olau Mountains of O'ahu, Hawai'i, from May 2013 to May 2014, while simultaneously studying their behavior at wind turbines within the broader landscape. This research aimed to assess the risk that wind turbines pose to bats on the island and integrated a variety of methods, including acoustic monitoring, thermal videography, and fatality searches. Our findings indicate that hoary bats were acoustically cryptic and occurred sparsely in the region. Overall site occupancy rate was 55% during the 1-year period of acoustic monitoring at 23 sites, and there was only an 8% chance of acoustically detecting a bat on a given night if it was present. We detected bats less frequently in windward northern parts of the study area and at windy, lower-elevation sites with rough terrain. Bats were detected more frequently in leeward southern parts of the study area and at wind-sheltered, higher-elevation sites with flat ridgetops. Acoustic detections were consistently low from October through February and increased at most sites to peak in April through August. However, meteorological conditions were not found to be associated with the acoustic prevalence of bats on a night-to-night basis.

We observed more than three thousand events involving bats during six months of nightly video surveillance at four wind turbines. Video monitoring revealed several links to weather at the local scale, despite acoustic detections not clearly relating to weather in our broader landscape analysis. Video demonstrated bats occurring near turbines more often on nights with little rain, warmer temperatures, moderate wind speeds, low humidity, and the low but rising barometric pressures indicative of fair weather and improved foraging conditions. Video monitoring also demonstrated that the presence of bats near turbines strongly correlates with insect presence.

We detected bats on video rather infrequently, averaging only one to two passes per hour. Most detections were brief (median = 4.0 sec) and involved single bats (97%), with the amount of time during which bats were observed totaling to only 0.10% of the video analyzed (about 3.8 hours of 3,847 total hours). Bats frequently foraged in the airspace near turbines. These results differ from a recent similar study on the mainland (continental North America) and may indicate that Hawaiian hoary bats spend less time closely approaching wind turbines and show less interest in them than their more-migratory mainland conspecifics. We speculate that the Hawaiian hoary bats we observed were locally resident and frequenting high-quality habitat near familiar structures. In contrast, hoary bats observed at wind facilities on the mainland appear to approach and investigate unfamiliar landscape structures that they mistake for trees as they migrate long distances. Consequently, Hawaiian hoary bats may be less susceptible to fatality at wind turbines on a per-encounter basis than hoary bats in North America. Only one bat carcass was found at the four turbines searched daily for six months. The relatively high probability of finding carcasses provided strong assurance that few carcasses were likely missed — there was less than a 10% chance that total fatality at the four turbines monitored for half a year exceeded three bats.

INTRODUCTION

The rapid expansion of wind energy nationwide is an important step toward reducing dependence on non-renewable sources of power. However, the magnitude of the wildlife impacts at wind energy facilities is a newly recognized threat, and the cumulative long-term impacts to various bat species are of increasing concern (Arnett et al. 2008, Boyles et al. 2011,

Kunz et al. 2007). It is estimated that tens of thousands of bat fatalities now occur each year at wind turbines in the U.S. and Canada (Arnett and Baerwald 2013), and migratory tree-roosting bats, including the genus *Lasiurus*, are consistently found at industrial wind turbines across North America in numbers that indicate the potential for rapid population declines.

The research presented herein focused on the Hawaiian hoary bat (*Lasiurus cinereus semotus*), a federally and state-listed endangered subspecies. Focus on the Hawaiian hoary bat was justified because of documented fatalities in the past five years on the islands of Maui, O'ahu, and Hawai'i (A. Nadig, U.S. Fish and Wildlife Service, pers. Comm.). The North American subspecies, *L. c. cinereus*, also accounts for approximately 40% of all bat fatalities at turbines in continental North America (Arnett and Baerwald 2013), and ancestral behaviors that potentially lead to susceptibility of populations in continental North America may still exist in the Hawaiian populations. The geographic setting is also appropriate because of the scope of active and planned wind energy development in response to an ambitious renewable energy mandate for Hawaii (70% clean energy by 2030; Braccio and Finch 2011).

The primary study objective was to assess the risk posed to Hawaiian hoary bats from wind turbines. To accomplish this we examined bat occurrence in relation to landscape attributes, meteorological conditions at both a regional scale as well as at a more local scale. Specifically, we examined acoustic samples of bat presence across a broad region to develop distribution models describing occurrence as a function of habitat and nightly weather conditions. In addition, we investigated bat activity immediately around wind turbines with thermal videography, and quantified its relationship to fine-scale temporal measures of weather conditions. We also examined the correlation of acoustic to visual (video) bat detections, and that of bat and insect co-occurrence. Finally, we searched for bat fatalities and estimated total fatality in the sample area during the study period.

METHODS

Study area

This study was comprised of two sample areas of different extents (Figure 1). The "regional" study of bat occurrence was conducted across a 56-km² area in the northern part of the Ko'olau Mountain Range that encompassed both public and private lands. The former included the Pupukeya-Paumalu Forest Reserve managed by the State of Hawai'i. The latter included the Kawailoa and the Kahuku military reservations administered by the U.S. Army but privately owned by Bishop Trust Estate and James Campbell Trust Estate. In addition, the study also included sample sites at facilities managed by Kahuku Wind Power (a subsidiary of First Wind, Boston, Massachusetts, USA, now SunEdison, Maryland Heights, Missouri, USA).

The "local" sample area of bat activity, behavior and potential fatality was centered at four wind turbine generators (WTG) managed by Kawailoa Wind Power (also a subsidiary of First Wind) on Oahu, Hawai'i, USA. We selected WTG 23, 24, 25, and 26 based on previous bat activity recorded at the site and logistics of securing video equipment. The Kawailoa facility consists of 30 2.3-Megawatt WTGs (Siemens SWT-2.3-101, Hamburg, Germany), with turbine towers 100 m (328 ft) in height with a rotor diameter of 108 m (354 ft) for a total height from base of tower to highest point of the blade of 154 m (505 ft).

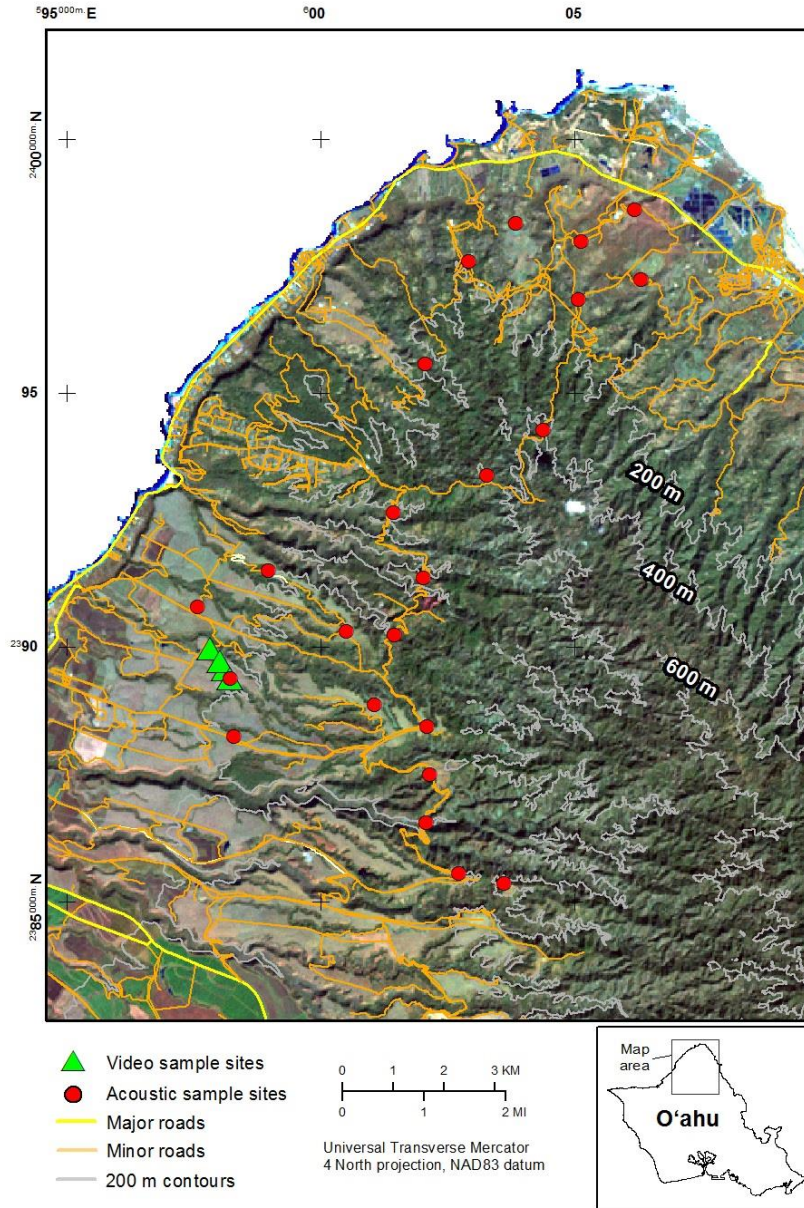


Figure 1. Acoustic and video sample sites on north O'ahu, Hawai'i.

Topography in the region consists of incised hillsides with elevation at sample sites ranging from 40 to 435 m (131 to 1,427 ft) above sea level. The area is dominated by a mix of agricultural lands (mostly pasture) and forest, with the latter extending across about one-half of the total region. Forest vegetation in the area is primarily introduced species of deciduous shrubs and trees at lower elevations and native species at higher elevations (generally above 200 m). Local climatic conditions are typical of lowland areas on O'ahu, with fairly constant temperatures and persistent light winds throughout much of the year. Annual temperature ranges from approximately 18.6 to 28.7 °C (65.4 to 83.6 °F, for the Waimea Arboretum located 3 km northwest of the nearest sample site; NOAA 2002). Annual precipitation reaches between 80 and 170 cm (31.5 and 67 in) along the elevation gradient of the study area (Giambelluca et

al. 2013). Prevailing northeasterly trade winds in the area generally blow from 19.8 to 28.8 km/hour (5.5 to 8 m/s; 12.3 to 17.9 miles/hour; AWS Truewind 2004).

Acoustic sampling and review

Acoustic data on the occurrence of bats were obtained from ground-based sources at 23 sites across the regional study area over a one-year period (May 14, 2013, to May 15, 2014; Figure 1). Although a probabilistic sampling involving a random selection of locations was initially planned, limited access and equipment security in much of the study region hindered its full implementation. Moreover, acoustic data was partly supplied by Kawaiiloa Wind Power (six of the 23 sites) and these locations were established before this study was initiated. Therefore, sites were selected for accessibility and broad coverage of the study region while maintaining a minimum spacing of 1 km. Departure from a probabilistic sampling design may bias model results (Rodhouse et al. 2011) and drawing inference to unsampled habitats should be treated with some caution; that is, inferences may be strongly suggestive but not conclusive.

Ultrasonic detectors (Song Meter SM2-BAT+, Wildlife Acoustics, Inc., Concord, Massachusetts) were used to acoustically record bat echolocation calls as a measure of nightly bat activity at each site. Detectors were equipped with SMX-US ultrasonic microphones which were positioned 2 - 4 m above ground. In addition, SM2-BAT+ ultrasonic detectors were mounted at the rear and on the bottom of the nacelles of WTG 23, 24, 25, and 26. Detectors were programmed to begin recording one hour before local sunset until one hour after sunrise the next morning. Acoustic recordings were recorded without compression as full-spectrum wav sound files with the following settings: sampling rate of 192 kHz; high pass filter at 1,000 Hz and + 36 dB gain; record microphone in mono; microphone bias off; Dig high pass filter at fs/24; Dig low pass filter off; Trg Lvl 18 SNR; Trig Win 2.0 sec; Trg Max Length 15 sec; Div Ratio 16; Nap Trg Lv1 off. Kaleidoscope Analysis Software (version 2.0.7; Wildlife Acoustics, Inc.) was used to filter background noise with the following settings: signal of interest (16-70 kHz); call/pulse duration (2–250 m/s); minimum number of calls/pulses (2). All files (inclusive of those classed as “noise”) were visually inspected as sonograms to ensure that there were no false positives and to determine the occurrence of terminal phase calls (“feeding buzzes”; Griffin 1958). Terminal phase calls were distinguished from search and approach phase calls by a rapid increase in the call rate.

Recording and review of video imagery

For a 6-month period (May 14 to November 14, 2013), bat occurrence and activity was monitored nightly at the local sample area comprised of four turbines (WTG 23, 24, 25, and 26; Figure 1) at the Kawaiiloa Wind Power facility. This time span was selected because it bracketed the period of peak acoustic activity (SWCA 2011) and the initial records of bat fatalities (A. Nadig, U.S. Fish and Wildlife Service, pers. comm.). This was accomplished using video surveillance cameras with sensors that operate in the ‘thermal’ spectrum of infrared light (approximately 9,000–14,000 nm; Model Q1922-E with a 35-mm lens, Axis Communications, Lund, Sweden) and which require no supplemental illumination. The effective sensor array size of the cameras was 640 x 480 pixels, and digital video was recorded at a rate of 30 frames per sec (fps) onto netbook computers (Model 1104 A7K67UT, Hewlett-Packard Company, Palo Alto, California, USA) equipped with external hard drives. Cameras were positioned 35 m from the base of each turbine so that they imaged about two-thirds of the rotor-swept zone (Figure 2). Video recording began within 1/2 hour of sunset and continued until approximately one hour after sunrise.



Figure 2. Video camera field-of-view.

Supplemental video imagery was also simultaneously recorded at three of the four turbines. At each of the three turbines we used a monochrome near-infrared (NIR) camera (Model KP-E500, Hitachi, Ltd., Tokyo, Japan) with a 1/2-inch interline electron-multiplying charge-coupled device (EMCCD) that provided a maximum sensitivity of 0.00003 lux and 640 x 480 pixel resolution, and equipped with a LMVZ990-IR lens with a 9–90 mm focal length and F1.8–F360 iris range. Each camera set-up included three NIR illuminators (Model T90A42, Axis Communications, Lund, Sweden). NIR imagery helped identify targets detected, judge spatial relationships between flying targets and the turbines, and gather additional details about behaviors of bats interacting with the turbine towers, nacelles, and blades. The NIR cameras and illuminators operate at range of light wavelengths (700–1,000 nanometers (nm)) not visible to bats (Hope and Bhatnagar 1979, Mistry and McCracken 1990). NIR cameras were positioned at 35 m from the base of each turbine and 3 NIR illuminators were positioned in an arc at 20 m from each turbine base (on the camera side) and aimed at the nacelle.

Video imagery was processed using custom code and matrix-based statistical software (Matlab with Image Processing Toolbox, Mathworks, Natick, Massachusetts, USA) to automatically identify frames with motion of small objects not associated with the moving turbine blades (Appendix 1). Although video was recorded at 30 fps, only every 30th video frame was analyzed due to time constraints on automated processing, resulting in detection of events lasting ≥ 1 sec. However, given the size of the field of view (FOV) and expected flight speed of hoary bats, few bats were likely missed given this sampling rate. That is, hoary bats fly at speeds ≤ 7 m/s (De La Cueva Salcedo 1995). Moreover, the size of the FOV was about 55 x 40 m given the camera resolution and the approximately 160-m maximum distance at which bats were detected. We estimate that a bat at that height would require at least seven seconds to fully

traverse the imaged area and would be detected in as many video frames. Therefore any bias associated with missing bats that passed through the video scenes in < 1 sec would involve those flying relatively close to the camera or at the edges of the FOV and not affect the detection of bats at nacelle height. Although spatial positions of objects are difficult to determine in two-dimensional video imagery, we were able to judge locations of bats in the airspace using target size, and thermal "silhouettes" (i.e., the thermal contrast of bats when passing on the camera side of the turbine), and shadows in the corresponding NIR imagery (e.g., bat passing close under bottom of nacelle).

All objects detected by software algorithms were visually reviewed and characterized as to identity and behavior. The identity of detections included bats flying around the turbines and rotor-swept zone, insects flying close to the cameras, and birds flying above the rotor-swept zone. Relative insect activity was derived from a tally of the number of sampled frames per hour in which insects were detected. For each detection of a bat in the thermal imagery we recorded the following behavioral information: time and duration of event, number of individuals present, predominant area of bat activity relative to direction the turbine nose was pointing (leeward, windward), height relative to the nacelle (above, below), flight path (straight, curved or erratic), whether the bat made very close approaches (approximately ≤ 4 m) to the turbine nacelle during the event, whether the bat appeared to be struck or displaced by a moving turbine blade, as well as descriptive comments about the event.

Habitat and weather data

Habitat data potentially associated with bat detection and distribution were obtained for the regional study area from geographic information system sources, and included canopy closure, landcover heterogeneity, elevation, terrain roughness, topographic position, and wind exposure. Forest canopy cover (percent) was obtained from the 30-m resolution Hawaiian Zone Tree Canopy Layer available from the National Land Cover Database (produced from 1999-2003 Landsat ETM+ scenes; version dated 10-28-08; http://www.mrlc.gov/nlcd01_data.php). Landcover heterogeneity was acquired from a 2.4-m resolution 2005 land cover map for the state produced by the Coastal Change Analysis Program of the National Oceanic and Atmospheric Administration (<http://coast.noaa.gov/digitalcoast/data/>). Landcover heterogeneity was derived by calculating the variety of landcover classes within 90 m of each raster pixel with the Spatial Analyst module of ArcGIS (version 10.2.2; ESRI 2014). For elevation data, we used a 10-m resolution digital elevation model (DEM) available from the USGS National Elevation Dataset (<http://ned.usgs.gov/index.html>). The terrain roughness index was calculated in ArcGIS as the difference between the elevation value of each 10-m DEM raster cell and the mean of an 8-cell neighborhood of surrounding cells (Riley et al. 1999). The index is unit-less, with high values representing topographically rough terrain. The index of topographic position classified the landscape into relative slope location, and was scaled from 0 (valley bottom) to 1 (ridge top), with mid-slope positions represented by intermediate values (De Reu 2013). Mean annual wind velocity at 100 m above ground level (<http://planning.hawaii.gov/gis/download-gis-data/>) was used to characterize wind exposure as a habitat attribute of an area. (Note that as an annual mean this metric differs from the nightly measures of mean wind speed).

Weather conditions were obtained from several sources located within the regional study area, including the nacelles of the four turbines monitored by video, a ground-based sensor close to these turbines, and a meteorological tower located about 1 km to the south of the turbines. These data were available for 10-minute intervals, and for analyses that used daily values the interval measures were converted to a nightly mean, median, or cumulative sum.

Meteorological data included temperature (Celsius), wind direction (median value calculated with the package 'circular' in program R (version 3.1.2; R Development Core Team 2011), wind speed (m/s), barometric pressure (mb), cumulative rainfall (mm), and humidity (%). Moon illumination was recorded as the proportion of lunar disk illuminated given that it was visible above the horizon. Because wind direction is a circular variable it was included in models as both a sine and cosine of the vector, in radians (Batschelet 1981). Moon illumination and sunrise/sunset data were acquired from the Astronomical Applications Department of the U.S. Naval Observatory (aa.usno.navy.mil/index.php). Julian date was included as an explanatory variable accounting for seasonal effects, and was converted to a sine function (Stolwijk et al. 1999) with its maxima (= 1) centered on June 25th, the period of peak bat detection. Sine values of 0 corresponded to September 25th and March 26th, and a sine of -1 corresponded to December 25th. This conversion allowed the modal pattern observed in bat detection to be shifted such that model intercepts need not be fixed on Julian day 1. The sine function also effectively reduced the number of factor levels from 365 (days) to 1, thereby improving model performance.

Bat fatality monitoring

Fatality searches

Fatality monitoring was conducted daily at the four turbines (WTG 23, 24, 25, and 26) concurrently monitored by video (15 May to 15 November, 2013). We delineated a rectangular plot 125 by 120 m for a total area of 15,000 m² centered on each turbine. We spaced transects 5 m apart and observers searched 2.5 m on each side of the transect line. We used a global positioning system (GPS; Trimble GeoXT, Trimble Navigation Limited, Sunnyvale, CA) to map the actual area searched for each turbine. Plots were mowed approximately every two weeks throughout the survey period to help maintain consistent vegetation height.

We conducted a "clean-out" search, in conjunction with our first search day, at each plot to remove any fatalities that may have occurred prior to 15 May. Searches were abandoned only when heavy rain, lightning, or turbine maintenance created a safety hazard, but resumed later that day if conditions permitted. When possible, searches commenced within 15 minutes of sunrise. We recorded date, start time, end time, turbine number, weather, and observer for each search. When a bird or bat carcass was found, the searcher placed a rock pile near the carcass, noted the time, contacted the crew leader, and continued the search. In most instances, the crew leader processed fatalities, but occasionally data were recorded by the searcher who found the carcass. After searching the entire plot, the searcher or crew leader returned to each carcass and recorded information on a fatality data sheet including date, species, sex and age (when possible), observer name, turbine number, perpendicular distance from the transect line to the carcass, distance from turbine, azimuth from turbine, visibility class of a one meter squared quadrat surrounding the carcass (Table 1), condition of carcass (entire, partial, scavenged), and estimated time of death (e.g., last night, 2 – 3 nights previously) based on condition of the carcass (e.g., eyes, smell, insects). Rubber gloves were used to handle carcasses, and all carcasses were placed in a labeled plastic bag and stored in an onsite freezer.

Incidental fatalities were defined as those found outside of the search plot, found in the search plot but outside the regular survey period, found in the search plot but determined to have died before the study was initiated (e.g., carcasses missed during "clean-out"), or found at an unsearched turbine. Carcasses found by the crew leader, who was not part of the search effort, were not considered incidentals if they were subsequently discovered by the designated

searcher. Incidental fatalities were reported to the crew leader and recorded on carcass data sheets, but were not included in analysis of fatality estimates.

Table 1. Habitat visibility classes of carcass search plots.

% Vegetative Cover	Vegetation Height	Visibility Class
≥ 90% bare ground	≤ 15 cm tall	Class 1 (Easy)
≥ 25% bare ground	≤ 15 cm tall	Class 2 (Moderate)
≤ 25% bare ground	≤ 25% > 30 cm tall	Class 3 (Difficult)
Little or no bare ground	≥ 25% > 30 cm tall	Class 4 (Very Difficult)

Field bias trials

Searcher efficiency and carcass removal rates were quantified to adjust the bat fatality estimate for bias caused by imperfect detection. Bias trials were conducted throughout the entire study period and at all sampled turbines, and searchers were never aware which turbines were used or the number of carcasses placed beneath those turbines during trials. We used a list of random turbine numbers, and random azimuths and distances (m) from turbines for placement of each carcass used in bias trials. We used freshly killed frozen rats as surrogates for the trials with the necessary assumption they were representative of bats (bat carcasses were not available for the trials).

Data recorded for each trial carcass included date and time of placement, carcass type, turbine number, distance and azimuth from turbine, and visibility class surrounding the carcass. Each searcher efficiency trial carcass was left in place and when possible checked after each search by another person who was not involved with the associated search. The day and time that each carcass was found was recorded by a searcher, then the carcass was marked with a rock pile and left in place to continue in the carcass persistence trial. If, however, a carcass was removed by a scavenger before a searcher had at least one opportunity to find the carcass (i.e., carcass not present before or after the first search was conducted) it was removed from the searcher efficiency trial and used only in the carcass removal data set. Thus, trial carcasses were available to be found on consecutive days during daily searches unless removed. For carcass persistence trials, carcasses were left in place until removed from the plot or at the end of the 20-day trial. Carcass condition was recorded daily for up to 20 days, as present and observable (1) or missing and or no longer observable (0). Each carcass was interval censored by time last seen (left censor) and time discovered missing (right censor), which allowed us to calculate carcass persistence from all carcasses used.

Data analyses

The analyses conducted for this study included assessments of bat distribution across the region, bat occurrence and behavior at turbines, and estimation of total bat fatalities. These analyses encompassed a range of spatial and temporal scales, and are separately described in the following sections.

Occupancy analysis of bat distribution

At a broad scale, occupancy analysis of acoustically-derived detections was used to examine the habitat and meteorological correlates of bat distribution (Gorresen et al. 2008). Nightly patterns of occurrence across the regional sampling area over a 1-year period were modeled to weather

data recorded for each 24-hour period (defined as starting at dawn on day 1 and running to dawn on day 2).

Conventionally, occupancy analysis uses multiple visits to a series of sites to create a history of encounters, and this is used to produce an estimate of the likelihood of detection that is in turn incorporated into an estimate of the proportion of sites occupied (MacKenzie et al. 2002). However, several lines of evidence indicate that Hawaiian hoary bats occur as year-round residents in the study area thereby making inference about site occupancy irrelevant because all or nearly all sites are likely occupied at one time or another during an annual period. The evidence includes preliminary acoustic samples in the region (SWCA 2010, 2011), turbine-related fatalities throughout the year (A. Nadig, U.S. Fish and Wildlife Service, pers. comm.), and the restricted elevation range on O'ahu that effectively limits the potential for altitudinal migration as observed seasonally on Hawai'i (Gorresen et al. 2013). Consequently, the prevalence of resident bats within the 56-km² study area on O'ahu was considered to be driven primarily by local conditions that vary over time (e.g., nightly and seasonal changes in weather, insect availability, etc.).

Whereas the spatial attributes of habitat that promote bat occurrence may be relevant for prospective planning and site selection, once turbines are installed the question accordingly shifts to what are the temporally varying conditions that affect bat presence (and thus risk) at one or more sites. Because the acoustic detectors were operated continuously and produced a relatively large sample size (i.e., up to 365 nightly samples at each of 23 sites), we were able to evaluate the temporally extensive dataset by applying a technique proposed by Weller and Baldwin (2012) that involved transposition of the encounter history matrix. Transposition resulted in rows comprised of nightly samples and columns consisting of sites, with the matrix populated according to whether bat passes were recorded or not recorded at each detector. Habitat attributes are subsequently interpreted as factors that affect variability in the local abundance and activity of bats in such a way as to make them more or less likely to be detected. In addition, meteorological parameters now become the focus of the occupancy analysis, with the large number of nightly samples providing relatively higher precision to the resulting occupancy estimates. These temporally variable parameters can then be interpreted as those affecting the regional prevalence of bats.

Because Hawaiian hoary bats were present year-round in the study area, we used a single-season occupancy model to quantify the underlying ecological process governing bat occupancy at sampled sites and the imperfect observation of such events (MacKenzie et al. 2003). Occupancy models were fit with the package 'Unmarked' (Fiske and Chandler 2011) in the program R. Models were comprised of two parameters describing the mechanisms underlying species occurrence: "occupancy probability" and "detection probability" (designated as ψ and p , respectively). Model notation included two forms for each parameter. For example, $\psi(\bullet)$ represented occupancy as a constant over all sample sites, and $\psi(\text{cov})$ denoted occupancy as a function of some covariate. Likewise, the notation $p(\bullet)$ indicated a detection probability parameter equal to the overall mean effect across sample sites, and $p(\text{cov})$ denoted the association of the parameter to one or more covariates. We used a null model, $\psi(\bullet)p(\bullet)$, that only included the intercept for each parameter as the basis for comparisons to models with site and sampling covariates. The null model also provided mean parameter estimates for all survey areas over the 1-year sampling period.

A set of preliminary models was developed separately for each of the two parameters wherein one parameter was modeled with covariates and the other parameter was treated as a constant: i.e., $\psi(\text{cov})\rho(\bullet)$ and $\psi(\bullet)\rho(\text{cov})$. The preliminary models were used to assess the effect of a single covariate on a particular parameter independent of its effects on other parameters (for example, $\psi(\text{temperature})\rho(\bullet)$ describes the effect of temperature on occupancy only). These "single-covariate" models were used only to identify candidates for use in more complex models, and included a total of six $\psi(\text{cov})\rho(\bullet)$ models and ten $\psi(\bullet)\rho(\text{cov})$ models. Within each set, a comparison of bias-corrected Akaike's information criterion (AIC_c) values were used to select the subset of preliminary models that provided the best fit to the data (Burnham and Anderson 2002).

Consideration of a model suite containing all possible combinations of ψ and ρ covariates was problematic because of the potential to over-fit models and yield Type I errors (Burnham and Anderson 2002). To limit the number of covariates tested, the building of more complex models was done in two steps. The first entailed selecting a subset of covariates from the preliminary models that were at least two AIC_c units less (i.e., "better") than the null model. Combinations of the resulting subset of five ψ and six ρ covariates produced a total of 31 $\psi(\text{cov})\rho(\bullet)$ models and 63 $\psi(\bullet)\rho(\text{cov})$ models. From each of these two separate sets, preliminary models within four AIC_c units of the top model were used as a candidate set to produce 12 final models that combined covariates for both the ψ and ρ parameters. Covariates initially considered for modeling were examined for correlation, and with one exception, the correlation coefficients for all covariates pairs were < 0.6. Measures of mean and maximum wind speed were highly correlated ($r = 0.98$); however, neither ranked sufficiently high nor were included in the final models.

To conduct goodness of fit tests, Unmarked provides the parametric bootstrapping function 'parboot' that simulates data from the fitted model and returns the Pearson's X^2 statistic (Fiske and Chandler 2011). Goodness-of-fit statistics were generated with 999 parametric bootstrap samples, and models with a X^2 p-value > 0.05 and an estimated over-dispersion parameter between 0.5 and 1.5 indicated an adequate model fit (MacKenzie and Bailey 2004).

All continuous covariates (except Julian date and wind direction which were already centered) were standardized to a mean of zero and unit variance to improve model convergence (Logan 2011). Standardization also permitted comparison of the relative effects of two or more explanatory variables that have different units of measurement, with estimated coefficients interpreted as a change in Y with an increase of one standard deviation in X while holding all other variables constant (Szumilas 2010). The R package 'AICcmodavg' (version 2.0-2; Mazerolle 2015) was used for model averaging and producing parameter estimates. We present the odds ratios, and detection and occupancy probabilities for the 12 final models. The covariate wind direction was described by two variables (sine and cosine) and the odds ratio was calculated as the mean of 1° increments in wind direction. Covariates with 95% confidence intervals (CI) for odds ratios which did not overlap 1, were considered to have a significant relationship with bat detection and occupancy patterns. In addition, the relationships are presented graphically from estimates produced by the 'predict' function in Unmarked. Unstandardized covariate values used in occupancy modeling are presented in Appendix 2.

Bat behavior at turbines

At the local scale, data acquired at the four turbines monitored by video were used to describe within- and between-night bat behavior over the six months of monitoring. For these

assessments, video detections of bats were treated as the same event when noted within one minute or less of other bat observations (1-minute intervals were arbitrarily chosen to facilitate rapid recording of time spans between detections).

Patterns of bat activity and occurrence observed by video were examined at two temporal resolutions — “instantaneous” and “nightly”. The former analysis was based on meteorological conditions recorded at 10-minute intervals, and related to bat occurrence tallied as “detected” or “not detected” for each time interval. The latter analysis entailed nightly averages of weather conditions and corresponding measures of bat detection rates, and provided an assessment of the response to conditions that bats would experience throughout the night. In contrast, the former approach provided an insight into conditions at the time of bat detection.

Kolmogorov–Smirnov (KS) tests were used to examine “instantaneous” patterns of bat detection in relation to univariate meteorological conditions recorded at 10-minute intervals. KS tests compared conditions (e.g., wind speed) during bat detections relative to intervals throughout the monitoring period when there were no bat detections (i.e., “ambient” conditions). To minimize the potential effect of large sample size on the p-value (Lin et al. 2013), ambient weather conditions were characterized by randomly subsampling the night-time 10-minute interval data to produce a sample size equivalent in size to the number of bat observations. KS tests were performed in program R.

Classification tree analysis was used to evaluate “instantaneous” patterns of bat detection in relation to multiple weather metrics. For this analysis we used a non-parametric approach to identify thresholds of meteorological conditions associated with detection rates. This was accomplished with the function “ctree” in the R package “party” (version 1.0-20; Hothorn et al. 2011). A model is built through recursive partitioning, a process in which a data set is split into groups based on homogeneity of response, then pruned to optimize the number of terminal tree nodes. Tree-based modeling can handle missing covariate values, both quantitative and qualitative covariates, and does not have the assumptions of generalized linear mixed models and neural networks (Olden et al. 2008).

Nightly patterns of bat activity and weather variables were examined with a regression tree analysis (Breiman et al. 1984). Detection rates were calculated as counts adjusted for variable survey effort; i.e., night duration and number of turbines monitored per night (to account for nights when video was available from only one turbine). The analysis was performed with the function “ctree” in the R package “party”.

Finally, bat detections were correlated to insect prevalence obtained from video at 1-hour increments. However, because the time of insect detection was only recorded to the hour, we were unable to adjust to account for seasonal changes in the length of night. Nevertheless, the data still allowed for direct hour-to-hour correlations in counts of bat and insect detections. These exploratory investigations used linear regression and correlation analyses, and were generally descriptive and qualitative in nature.

Bat fatality monitoring

Bat fatalities were sought daily at the four turbines monitored by video, and the expected total fatality during the 6-month monitoring period was estimated using a model that accounted for the imperfect detection of carcasses.

Carcass Persistence: Estimates of the probability that a bat carcass was not removed in the interval between searches were used to adjust carcass counts for removal bias. Removal was defined as a carcass not present within the searchable plot (i.e., removal by scavenging, wind, water, etc.). Since we did not know the exact time a carcass was removed, the data were considered interval censored between the last time known present and first time known absent. The length of time a carcass remained in the survey area before it was removed can be modeled as an exponential, Weibull, log-logistic or log-normal distributed random variable. We fit carcass persistence time data to each of these failure-time models with and without visibility class as a covariate and used AIC_c model selection (Burnham and Anderson 2002) in the Fatality Estimator software (Huso et al. 2012) to determine the best model. To increase our sample size, we made the assumption that carcass persistence did not vary significantly for a particular turbine and we used carcasses from all turbines to calculate carcass persistence. We also assumed that the use of rats (*Rattus norvegicus*) as surrogate carcasses were representative of bat fatalities (Hawaiian hoary bat carcasses were not available for carcass persistence and searcher efficiency trials).

Searcher Efficiency: We used estimates of the probability that a carcass will be seen by an observer during a search to adjust carcass counts for observer bias. The failure of an observer to detect a carcass on the search plot may be due to its size, color, or time since death, as well as conditions in its immediate vicinity (e.g., vegetation density, shade, etc.). Based on results of 12 studies conducted throughout the U.S. (Schirmacher, pers comm.) and consistent with findings of Warren-Hicks et al. (2013), we assumed that a carcass's "observability" decreased by a factor of 0.67 with each search. After accounting for carcasses removed before a searcher had the chance of observing them, data from searcher efficiency trials were fit separately to a logistic regression model using the Fatality Estimator software (Huso et al. 2012). The odds of observing a carcass on the first search were modeled with and without visibility class as a covariate. We used AIC_c to select the best model (Burnham and Anderson 2002). To increase our sample size, we made the assumption that searcher efficiency was more related to visibility class and not related to turbine location, and thus all applicable carcasses from all turbines were used.

Fatality estimation: Currently available approaches for estimating fatality from observed carcasses (e.g., Korner-Nievergelt et al. 2011, Huso et al. 2012, Korner-Nievergelt et al. 2012, Warren-Hicks et al. 2013) are fairly robust when observed counts are high, but can only estimate 0 fatality with no variance when no carcasses are observed, and can be inaccurate when observed counts are low. Huso et al. (In press) developed an approach that uses Bayes' formula to calculate credible intervals for actual mortality when zero or only few carcasses are observed. Calculations for this approach are available in Evidence of Absence v1.00 software (Dalthorp et al. 2014) and all fatality estimates were calculated using this software.

RESULTS

Occupancy analysis of bat distribution

The Hawaiian hoary bat was acoustically detected during 327 of 7,176 detector-nights across 23 sites over the 1-year study period (where detector-nights are the total number of sampling nights with operating detectors). Mean detection probability across all survey sites for the 1-year period was 0.08 (95% CI = 0.07 to 0.09), where a \hat{p} value of 1.0 indicates detection at all nights. Mean occupancy of all survey sites for the 1-year period was 0.55 (null model 95% CI =

0.48 to 0.62), where a $\hat{\psi}$ value of 1.0 indicates bat detection at all sites. There were considerable differences among survey sites in the proportion of nights by month with bat detections (Figure 3). Nineteen of the 23 sites had an observed detection probability less than or equal to the predicted mean of 0.08, including two sites with no detections throughout the entire 1-year period (Figure 4). Acoustic recordings were obtained for an average of 85% of the nights sampled (range: 30–100%). Recordings were unavailable for some sites and nights because of power failure (battery theft and inadequate solar exposure to the photovoltaic panels), compact flash card corruption and other undetermined problems.

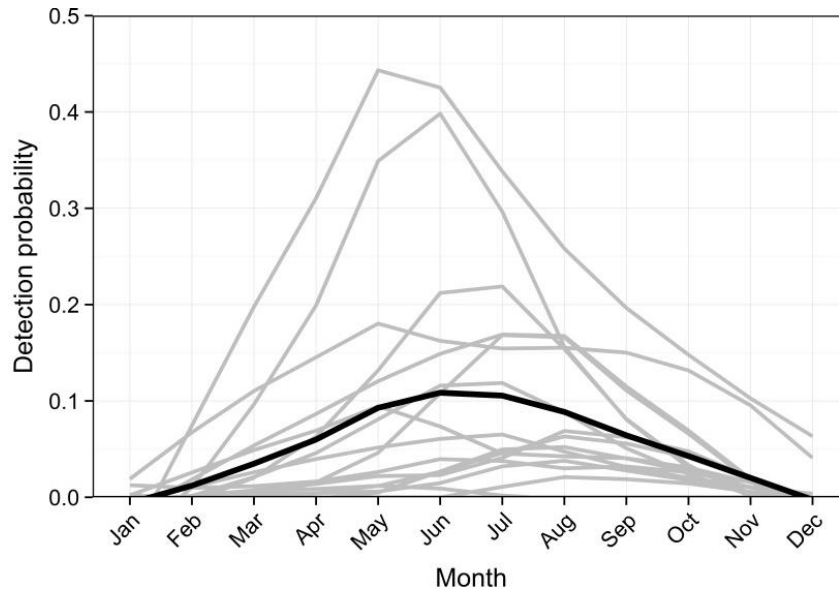


Figure 3. Observed nightly bat detection probability by month among survey sites. Sites depicted include only those for which surveys were conducted in all months ($n = 19$) and curves were produced with loess smoothing. Detection probability averaged for all survey sites is shown in black.

The evaluation of preliminary single-covariate models identified a suite of variables associated with detection probability (weather metrics) and occupancy (habitat attributes). All habitat attributes and several weather metrics were included in preliminary models that performed better than the null model (i.e., model with no covariates; Appendix 3). Model selection further produced 12 top-ranked models used for model averaging and parameter estimation. Models with low weights contributed a proportionally small amount to model averaged parameter estimates and were retained only for illustrative purposes. The final models for explaining the acoustic detection of Hawaiian hoary bats had AICc weights ranging from 0.01 to 0.29 indicating relatively high model uncertainty (Appendix 4). Nevertheless, several covariates were consistently represented in all or most models. Julian date and temperature were included as ψ covariates in all models. The inclusion of Julian date was expected given that the sine function describing this variable was centered on periods of highest and lowest bat detection across the region (late June and late December, respectively), but it also confirms that there were strong time-of-year effects on bat distribution. Mean daily temperature, in combination with Julian

date, demonstrated a strong relationship with the seasonal prevalence of bats across the sample sites (Table 2). The final model predicts that bats are more widespread in summer months and during nights with a higher mean temperature compared to winter months and nights with a lower mean temperature (Figure 5). Besides Julian date and temperature, all other weather metrics demonstrated a weak to negligible association with the prevalence of bats across the sample sites (Table 2). These relationships are presented in Figures 6 to 8 for illustrative purposes only.

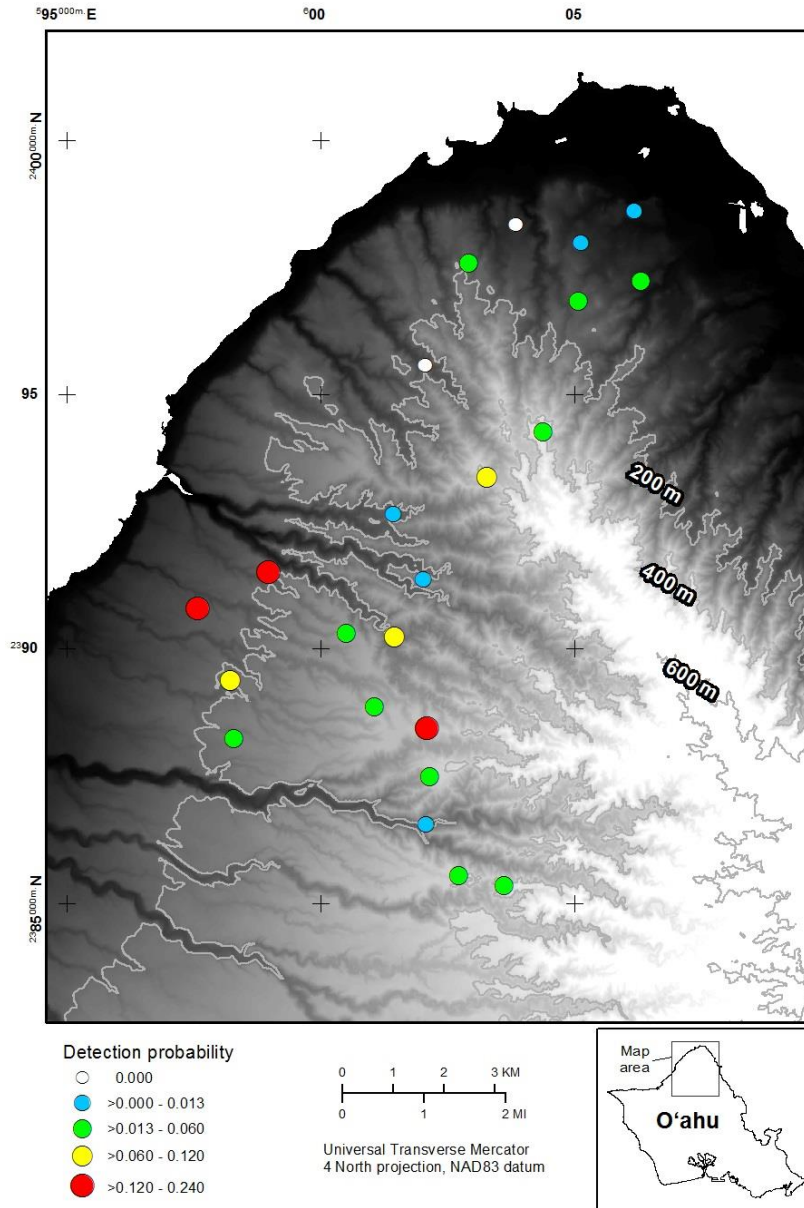


Figure 4. Observed nightly bat detection probability by survey site as averaged for the 1-year acoustic survey period.

Table 2. Model-averaged coefficient estimates, unconditional standard errors, and odds ratios with 95% confidence intervals (CI) for the parameters identified in the set of 12 final models (Appendix 4). Covariates with 95% CIs for odds ratios which did not overlap 1 were considered to have a significant relationship with bat detection and occupancy patterns.

Model parameter	Covariate	Coefficient (logit scale)	SE	Odds ratio	Lower 95% CI	Upper 95% CI
ψ	Julian date	2.702	0.438	14.907	6.317	35.174
ψ	temperature	0.736	0.213	2.087	1.374	3.169
ψ	barometric pressure	-0.302	0.261	0.740	0.444	1.233
ψ	relative humidity	-0.272	0.224	0.762	0.492	1.181
ψ	wind direction (sine)	-0.536	0.343	1.310 [†]	0.618 [†]	2.783 [†]
ψ	wind direction (cosine)	0.710	0.396			
ρ	elevation	0.289	0.092	1.335	1.115	1.600
ρ	topographic position	0.285	0.076	1.330	1.146	1.543
ρ	terrain roughness	-0.334	0.129	0.716	0.556	0.923
ρ	wind exposure	-0.299	0.084	0.741	0.629	0.874
ρ	canopy cover	-0.190	0.106	0.827	0.673	1.017
ρ	landcover heterogeneity	-0.074	0.096	0.928	0.770	1.120

[†] calculated as the mean of odd ratio values for sine and cosine parameters of wind direction

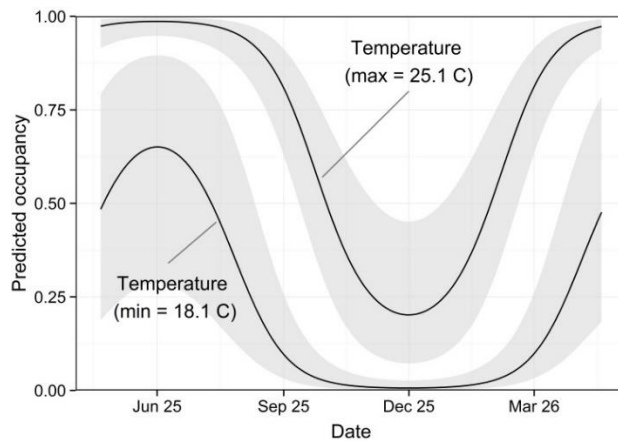


Figure 5. Occupancy of Hawaiian hoary bats as a function of time of year and mean nightly temperature (which ranged from 18.1 to 25.1 °C for the 1-year study period).

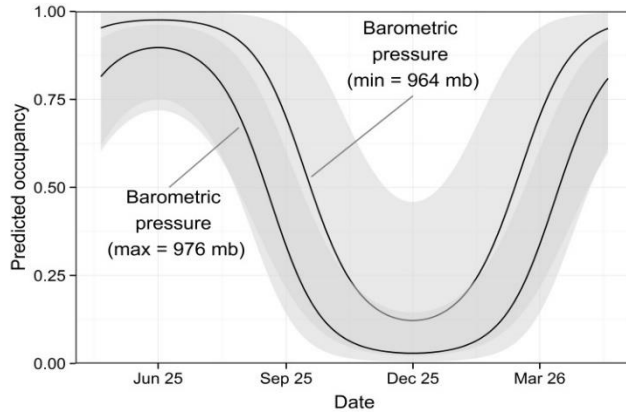


Figure 6. Occupancy of Hawaiian hoary bats as a function of time of year and barometric pressure (which ranged from 964 to 976 mb for the study period).

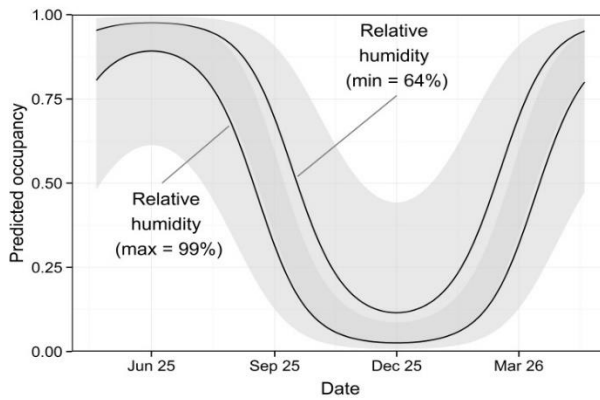


Figure 7. Occupancy of Hawaiian hoary bats as a function of time of year and mean nightly relative humidity (which ranged from 64 to 99 percent for the 1-year study period).

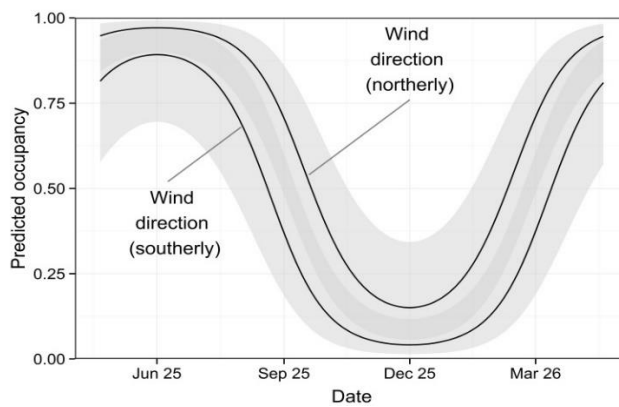


Figure 8. Occupancy of Hawaiian hoary bats as a function of time of year and wind direction (for graphical clarity, shown here only for northerly and southerly prevailing winds).

The covariates most strongly associated with detection probability included elevation, wind exposure, topographic position, and terrain roughness (Table 2). With the exception of terrain roughness, these covariates were represented in all 12 of the final models (Appendix 4). The models demonstrated that bats were less detectable in lower-elevation habitats and in areas exposed to higher mean annual wind speeds compared to higher elevations and low wind exposure areas (Figure 9). In general, this reflects the north-south axis of detection probability in which the more southerly sites tended to be at higher elevations and more sheltered from prevailing winds (Figure 4). Detection probability was also associated with landscape features, in that bats were less frequently encountered acoustically in valley bottoms and uneven terrain compared to ridge tops and even terrain (Figure 10). Although only marginally significant, canopy cover was negatively related to bat detection (Figure 11), and indicates that Hawaiian hoary bats frequent open habitats with little tree cover. Landcover heterogeneity was negligibly associated with detection. Several other occupancy covariates were excluded or were under-represented in the final models. These included moon illumination, precipitation, and wind speed (mean, variability, and maximum). All of these covariates had AIC_c values greater than or within two units of the null model (i.e., model without covariates) meaning that they provided little to no explanatory power.

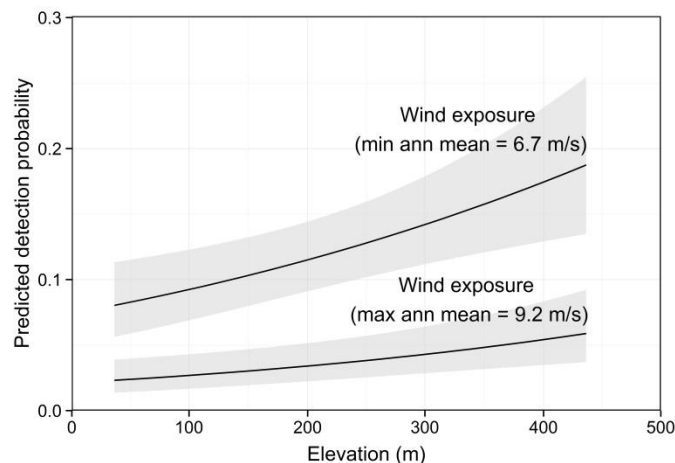


Figure 9. Probability of detecting Hawaiian hoary bats as a function of elevation and wind exposure (annual mean wind speed ranged from 6.7 to 9.2 m/s across the study region).

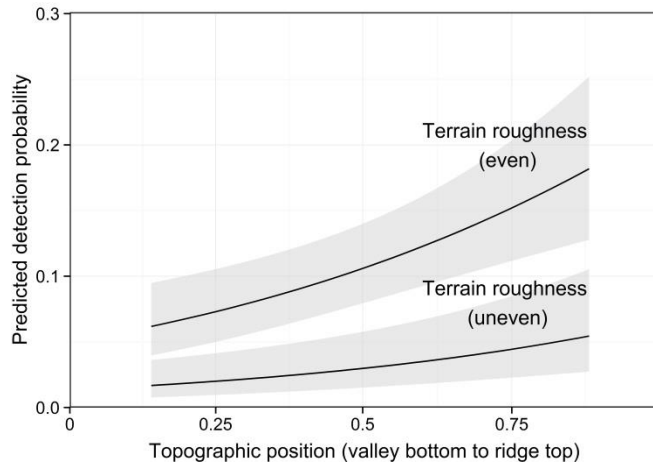


Figure 10. Probability of detecting Hawaiian hoary bats as a function of topographic position and terrain roughness.

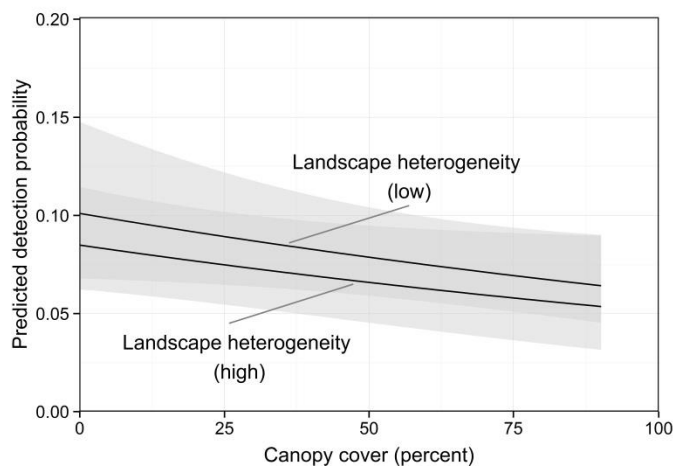


Figure 11. Probability of detecting Hawaiian hoary bats as a function of canopy cover and landcover heterogeneity. Both variables demonstrated weak to negligible association with detection probability.

Bat behavior at turbines

Over the 6-month study period, we recorded 8,080 hours of video at the four turbines monitored by thermal surveillance cameras. This yielded 682 turbine-nights with a full night of recording (average duration = 10.8 hours). Because of the large amount of video recordings and high bat detection rate (compared to a previous study in Indiana [Cryan et al. 2014a]), we systematically subset the recordings to process and analyze the video from two turbines per night (where available). Review of 339 turbine-nights (3,847 hours) of video resulted in 3,388 observations of bats (86%), 498 bat-like detections (13%), 32 bird detections (1%), and numerous insect detections. Only definitive bat detections were used in analyses of occurrence and behavior (i.e., bat-like detections were not included). To facilitate tallying the high number

of insect detections this metric was recorded as frequency of detections by hour (rather than exact time of detection).

Video detections of bats at turbines occurred throughout the night but were generally bimodal with peaks about 2–3 hours after sunset and 4 hours before sunrise (Figure 12). Bats were detected throughout the 6-month monitoring period and demonstrated little evidence of a seasonal shift toward earlier or later activity as a function of time of night ($P = 0.3120$; Figure 13). The hourly rate of nightly bat detection (number/hour/turbine) was highly variable but significantly increased ($P = 0.0001$) from a mean of 0.5 on survey day 1 (May 14) to a mean of 1.2 on survey day 185 (November 14) over this period (Figure 14). The mean number of nightly detections per turbine (adjusted for duration of night) for the entire study period was 9.5 (min: 0; 1st qu.:3; median: 7.3; 3rd qu.: 13; max: 67).

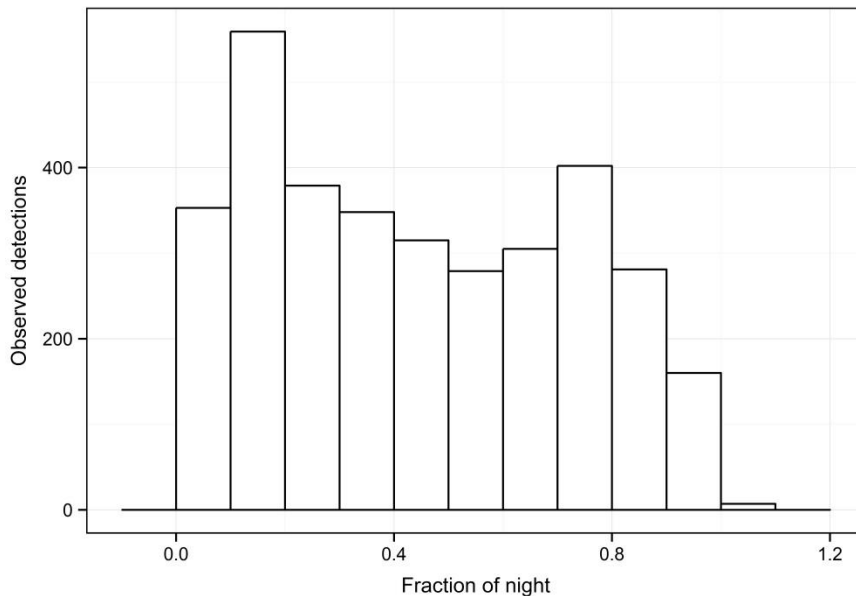


Figure 12. Observed distribution of video detections of bats by time of night. Data are compiled for all nights over the 6-month monitoring period. To account for seasonal changes in the length of night, the time of detection was standardized as the fraction of night (with dusk = 0.0 and dawn = 1.0).

Almost all (97%) bat detections involved single bats within the 1-minute period used to quantify each event (Figure 15). Multiple bats (that is, those seen concurrently) were observed very infrequently, with two and three bats observed during 2.7% and 0.2% of all detections, respectively, and four and five bats observed only once each (0.03%). Bats were rarely seen chasing or following each other, although on two occasions within a single night (November 14), multiple bats were seen hovering near and chasing one another for extended periods (95 seconds and 360 seconds).

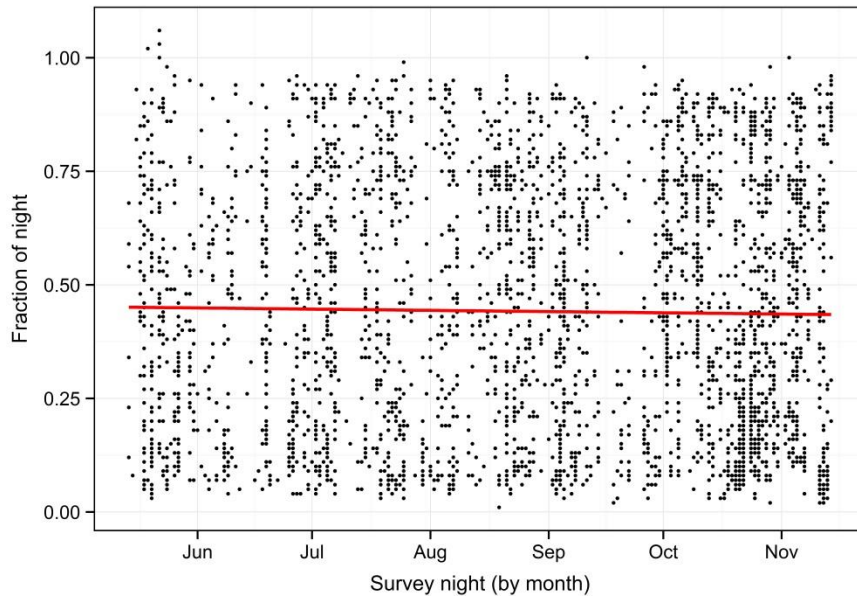


Figure 13. Video detections of bats by time of night over the 6-month monitoring period. To account for seasonal changes in the length of night, the time of detection was standardized as the fraction of night (with dusk = 0.0 and dawn = 1.0). The red line is a linear model of trend in detections as a function of time of night.

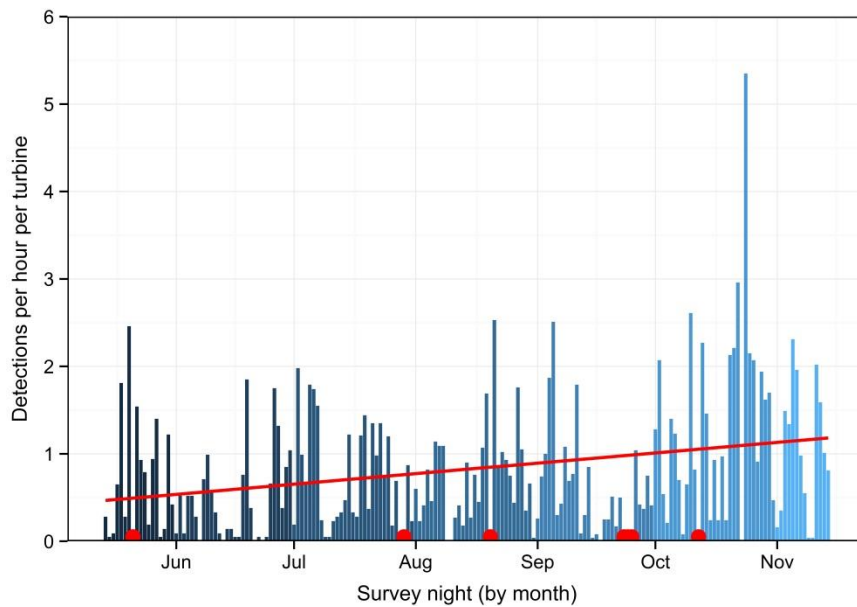


Figure 14. Video detections of bats per hour by night over the 6-month monitoring period. Detections are adjusted by survey effort (i.e., night duration and number of turbines monitored per night). The red line is a linear model of trend in detection rate over the monitoring period (excluding nights with no samples as indicated with red points).

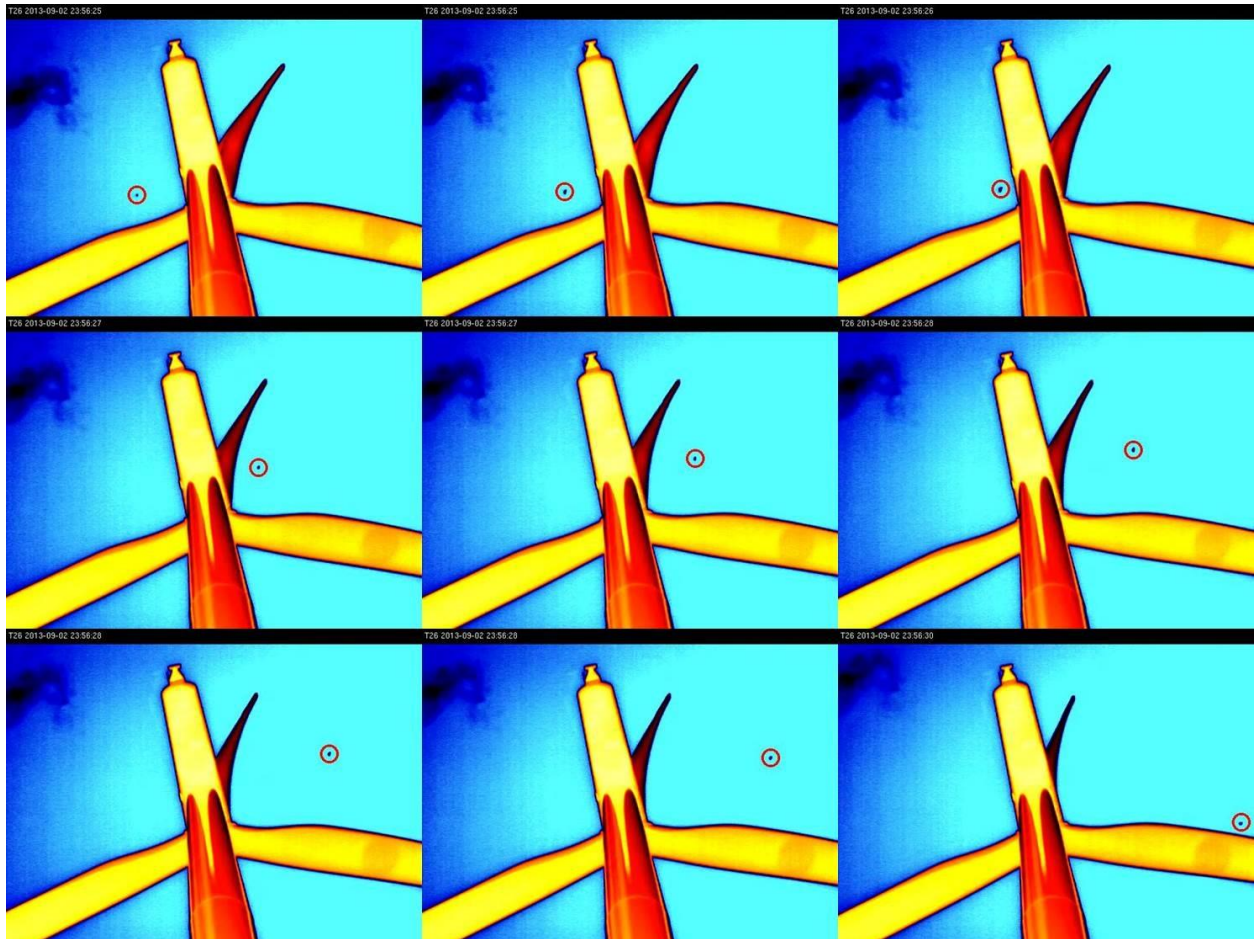


Figure 15. Example of a bat detection from a thermal video image sequence at approximately half-second intervals (left to right; top to bottom).

The durations of most bat detections were relatively brief given the small field-of-view (Figure 16), and averaged 4.0 seconds per event (min: 0.1; 1st quantile: 1.6; median: 2.4; 3rd quantile: 3.6; max: 360.0). However, 10% ($n = 335$) of the detections lasted 6.3 seconds or more, with 10 detections lasting ≥ 60 seconds, and one detection of 5 bats sustained for at least 360 seconds. Adjusting for the number of turbines monitored, on nights with bats detections the cumulative duration of detections averaged 41.9 seconds (min: 0.3; 1st quantile: 9.7; median: 27.9; 3rd quantile: 57.6; max: 551.6). The mean duration of detections per night marginally increased ($P = 0.0265$) from 2.6 on survey night 1 (May 14) to 3.9 seconds on survey night 185 (November 14; Figure 17). However, bats generally did not appear to be spending much time in the rotor-swept zone imaged by video. Cumulatively, the amount of time during which bats were observed totaled to only 0.10% of the video analyzed (about 3.8 hours of 3,847 total hours).

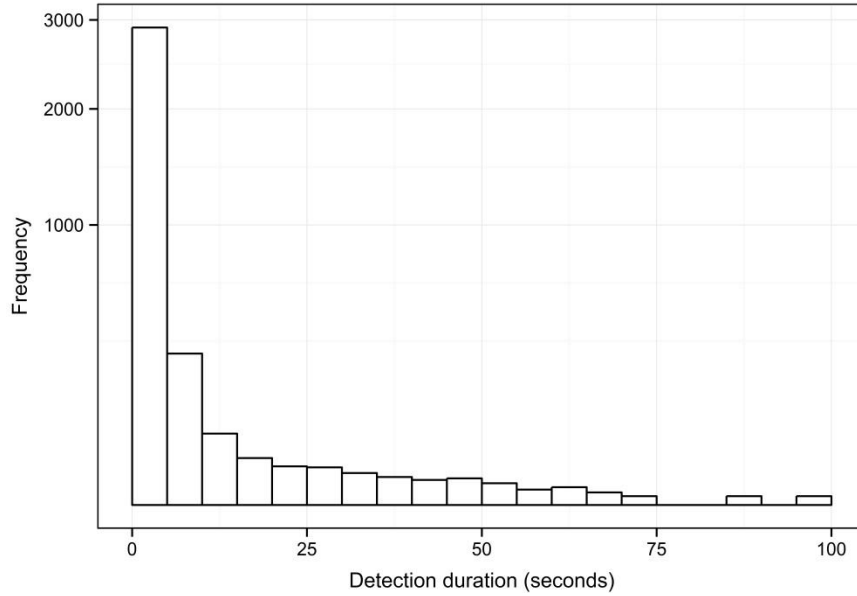


Figure 16. Frequency of the duration of video detections of bats (sec) in the video field-of-view. For graphical clarity an outlier observation of 360 seconds was not included.

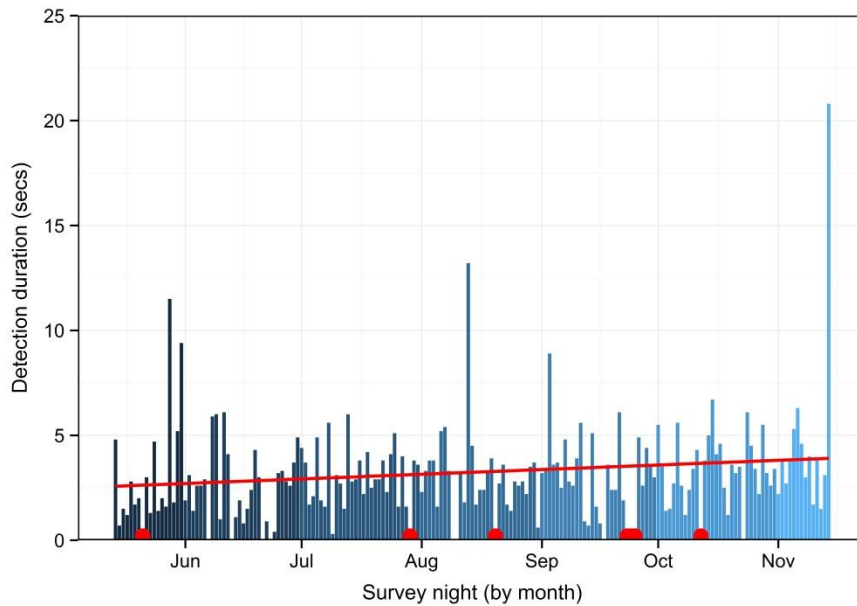


Figure 17. Mean duration (sec) of video detections of bats over the 6-month monitoring period. Detections are adjusted by survey effort (i.e., number of detections and turbines monitored per night). The red line is a linear model of trend over the monitoring period (excluding nights with no samples as indicated with red points).

Most (86%) detections were of a bat making a single pass through the field of view within a 1-minute period of observation. Repeated passes were seen less frequently: 2 (9%), 3 (2%), 4 (2%), 5 (0.7%) and 6 (0.2%) passes. The largest proportion of bat detections involved erratic (41%) flight indicative of active foraging behavior in the immediate area of the turbine. Curved flight trajectories that may have comprised either an approach to or avoidance of the turbine were made 22% of flight passes. Straight flight paths indicative of a “fly-by” were observed in 38% of detections. Some of the observed curved and straight trajectories may simply consist of the less erratic parts of flight by bats otherwise engaged in foraging.

The majority of bat detections appeared to be of individuals within the rotor-swept zone (70%) or within about 4 m (16%) of the turbine nacelle. The remaining detections (14%) were of distant bats (approx. > 150 m) above or behind the rotor-swept zone. Most bats (70%) also were observed flying below the nacelle, with a smaller portion (30%) above the nacelle. The proportion of leeward versus windward detections was about 74% and 17%, respectively, with the remaining 9% of detections of a bat traversing both areas. However, these proportions may not be directly comparable given that the likelihood of detecting bats diminishes with distance and the airspace volumes sampled were not equal. That is, the video cameras provided an upward angle of view that was narrower near the ground (i.e., an inverted pyramid; Figure 2), and offered a closer perspective of leeward activity than that of windward activity. The prevalent easterly wind direction also favored a leeward view. Nonetheless, the observations do demonstrate that there is considerable nightly activity in areas at which bats may be at risk of strikes by rotating blades. Observations of displacement of bats by spinning turbine blades were seen in 23 cases (0.7%), with “near strikes” noted in 8 cases (0.2%). Direct strikes of bats by turbine blades were not observed. The single bat fatality located during ground-searches (see Results section “Bat fatality monitoring”) is believed to have occurred when the video cameras were not operating because of electrical grid maintenance.

A graphical comparison of nightly bat detection rates to a time-series of weather variables indicated that higher rates generally occurred when nightly mean wind speed dropped to a low relative to the previous night and temperatures were relatively high (Figure 18). Kolmogorov–Smirnov (KS) tests confirmed that bats were more likely to be present when mean wind speeds were < 4.6 m/s (KS test, $D = 0.1992$, $P < 0.0001$; Figure 19) and when temperatures were > 22.2 °C (KS test, $D = 0.1181$, $P < 0.0001$; Figure 20). The positive relationship of the latter appears mostly driven by increase in nightly temperature during summer.

The approach of storms is generally associated with rapid changes in barometric pressure. The effects of this variable on bat activity were examined in two ways. The first entailed a comparison of activity to conditions observed during the night of sampling. A KS test demonstrated that bats were more likely to occur when barometric pressure was relatively low (≤ 972 mb; KS test, $D = 0.0624$, $P < 0.0002$; Figure 21). The second involved a comparison of activity relative to the trend in barometric pressure (rather than the actual value itself). Trends were quantified by fitting a spline to barometric pressure (Figure 22) and calculating the first derivative of the spline (i.e., slope of the trend), where negative and positive trends demonstrate a drop or upturn in pressure during the night, respectively. A KS test found a significant and positive relationship between the frequency of bat detection and the current night’s trend in barometric pressure (KS test, $D = 0.0627$, $P = 0.0002$; Figure 23). However, marked and sustained changes in barometric pressure typically occurred over a period of

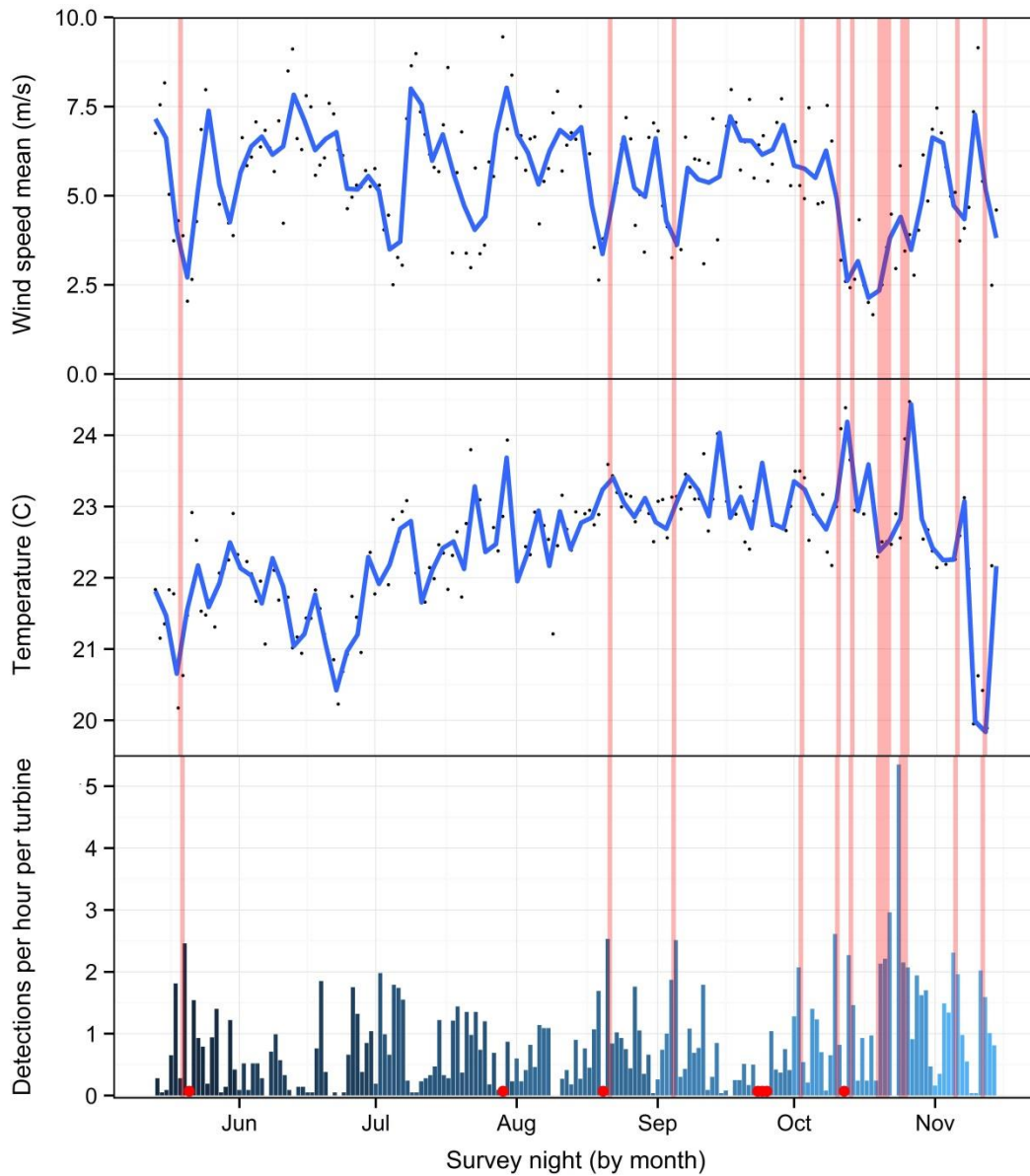


Figure 18. Correspondence between the rate of bat detections and mean nightly wind speed (m/s) and temperature (°C). Detection rate is adjusted by survey effort (i.e., night duration and number of turbines monitored per night). As a visual guide the vertical red bars align peak detections (arbitrarily chosen at ≥ 2 per hour per turbine) with weather variables. The blue lines are splines fit to wind and temperature data. Red points indicate nights with no available video samples of bat activity. Higher detection rates occurred when nightly mean wind speed dropped to a low relative to the previous night and temperatures were relatively high.

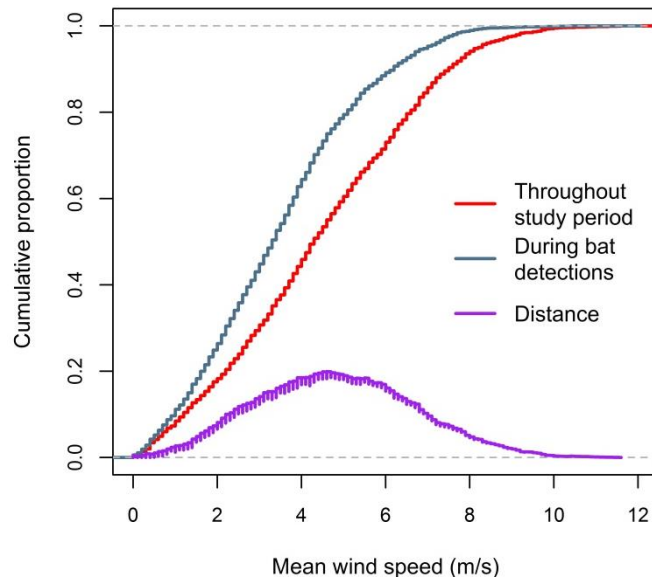


Figure 19. Cumulative distribution functions of mean wind speed during video detections of bats relative to conditions recorded throughout the monitoring period when no bats were detected. Distance values (the absolute difference at any interval between the pair of functions for each of the two samples) indicate conditions during which bats were detected more or less frequently than expected. Increasing distance values indicate relatively more-frequent observations than expected where the function for bat observations occurs above the function for “ambient” conditions. Bats were more likely to be present when mean wind speeds were < 4.6 m/s.

several nights (Figure 22). Therefore, bat occurrence was also tested against the trend in pressure of the preceding night. The frequency of bat detection was also found to be significantly and positively related to barometric pressure trend over the previous 24-hour period (KS test, $D = 0.0700$, $P < 0.0001$; Figure 24). That is, bats were more likely to occur following periods when barometric pressure had declined and was near or at a low and beginning to increase over at least one 24-hour period (with the range of trend slope values spanning -0.02 to 0.08). Bats were also more prevalent when maximum wind speeds were < 8.2 m/s (KS test, $D = 0.2018$, $P < 0.0001$; Figure 25), and during periods with little or no rain (Figure 22, and analyses further below). Taken together, these results indicate that relatively higher bat activity occurred as storm fronts passed and weather conditions were improving. Moon illumination was found to be only marginally related to the frequency of bat detections (KS test, $D = 0.0387$, $P = 0.0593$; Figure 26), with slightly higher activity at low illumination levels.

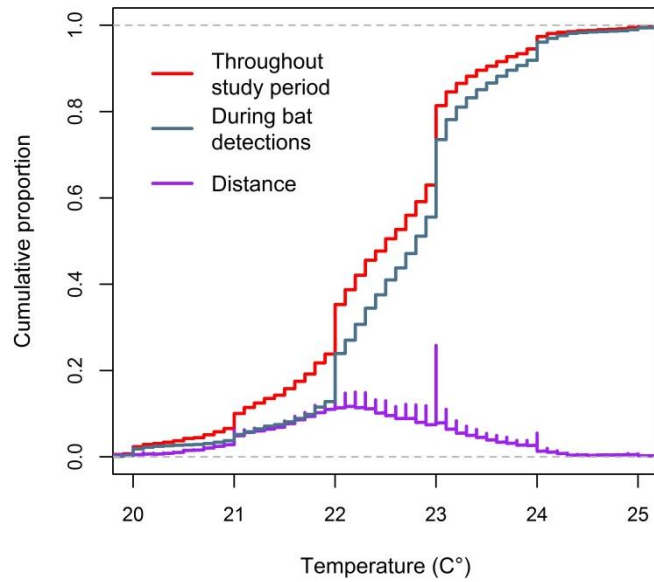


Figure 20. Cumulative distribution functions of mean temperature during video detections of bats relative to conditions recorded throughout the monitoring period when no bats were detected. Decreasing distance values indicate relatively more frequent observations than expected where the function for bat observations occurs below the function for “ambient” conditions. Bats were more likely to be present when temperatures were > 22.2 °C.

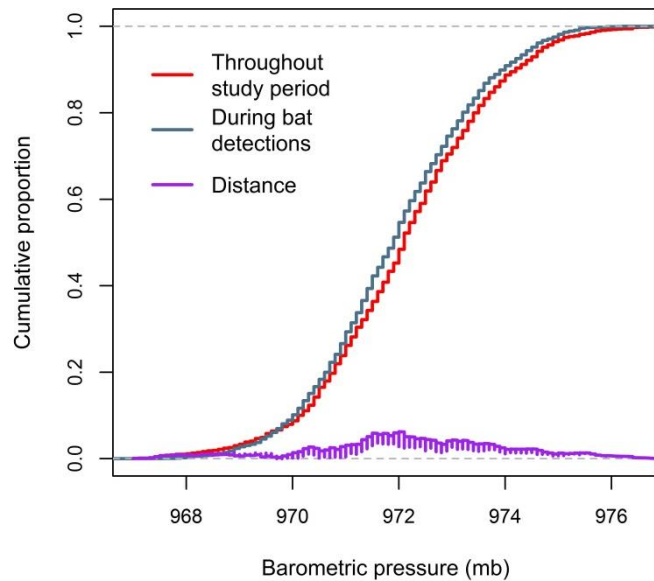


Figure 21. Cumulative distribution functions of nighttime barometric pressure during video detections of bats relative to conditions recorded throughout the monitoring period when no bats were detected. Bats were more likely to be present when barometric pressure was ≤ 972 mb.

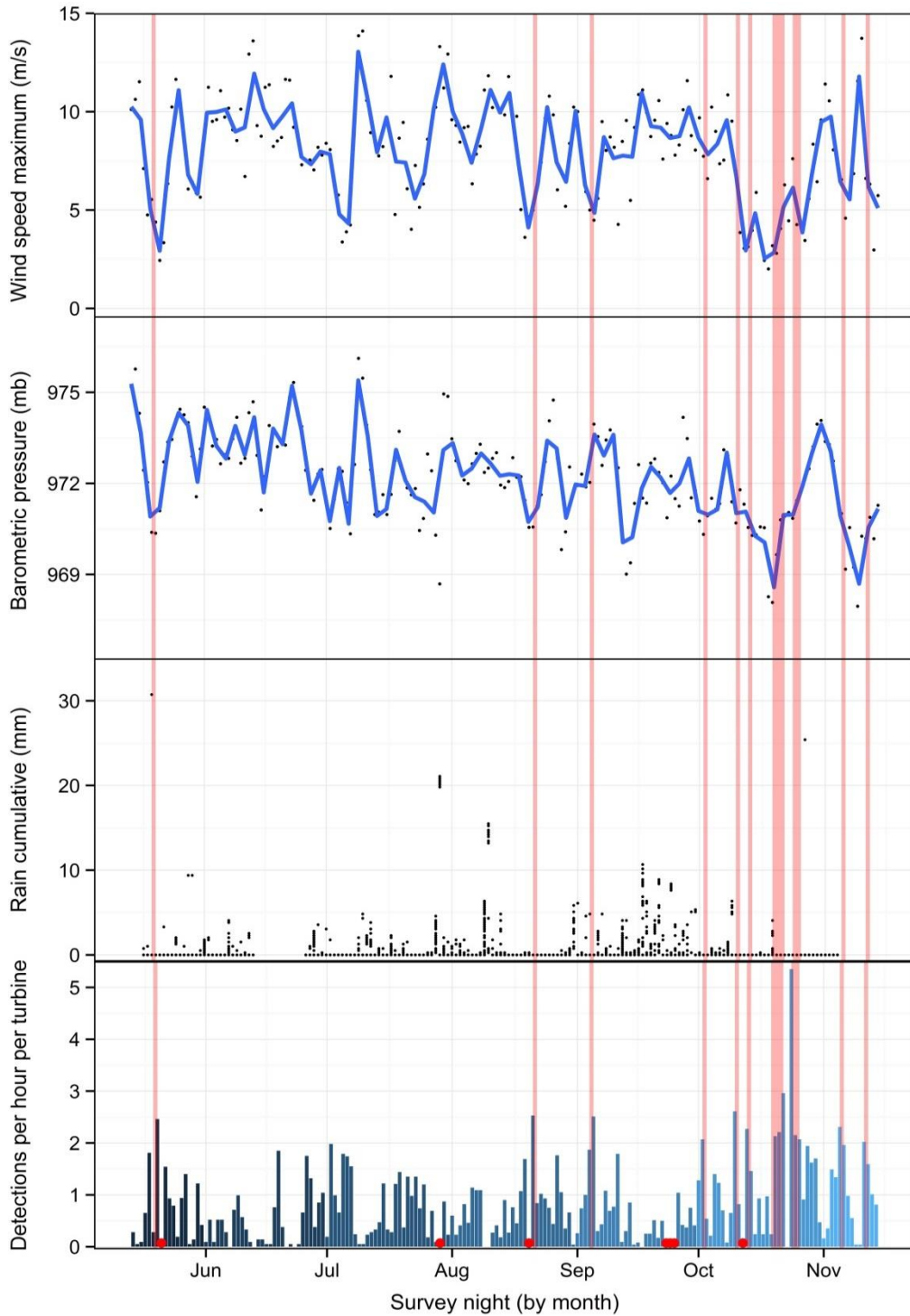


Figure 22. Correspondence between the rate of bat detections and maximum wind speed, barometric pressure, and cumulative rainfall. Detection rate is adjusted by survey effort (i.e., night duration and number of turbines monitored per night). As a visual guide the vertical red bars align peak detections (arbitrarily chosen at ≥ 2 per hour per turbine) with weather variables. The blue lines are splines fit to barometric pressure and wind speed data. Red points indicate nights with no available video samples of bat activity.

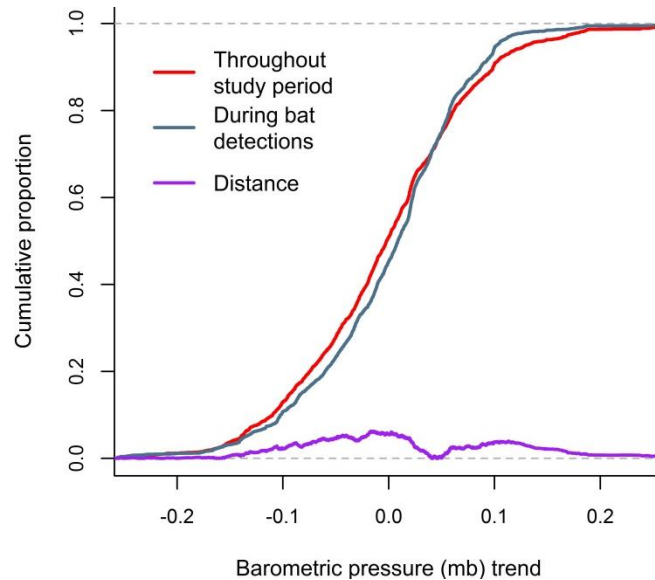


Figure 23. Cumulative distribution functions of barometric pressure trend during video detections of bats relative to conditions recorded throughout the monitoring period when no bats were detected. Note that decreasing distance values indicate relatively more frequent observations than expected where the function for bat observations occurs below the function for “ambient” conditions. Conversely, increasing distance values indicate relatively more frequent observations than expected where the function for bat observations occurs above the “ambient” function. Consequently, the range of trend values during which bats were more frequently detected span -0.01 to 0.12 corresponding to the beginning of an increase in barometric pressure during the current night of sampling.

Classification tree analysis of observations recorded at 10-minute intervals provided insight into bat occurrence patterns given “instantaneous” weather conditions (i.e., those recorded at the time of observation). The analysis identified gusty, cool, and humid conditions to be negatively associated with bat occurrence (Figure 27). The path that favored the highest proportion of bat detections included conditions where maximum wind speeds were ≤ 7.7 m/s (or between 7.7 and 8.7 m/s with temperatures > 21.5 °C). The path that favored the lowest proportions included humidity levels $> 90.0\%$ and maximum wind speeds > 8.7 m/s, or humidity levels $\leq 90.0\%$ and maximum wind speeds > 12 m/s. Proportion of detections were also low where wind speeds were between 7.7 and 8.7 m/s and temperatures were ≤ 21.5 °C, reflecting the seasonal patterns of lower bat occurrence prior to the late summer months when bats were less frequently detected by video (Figure 18).

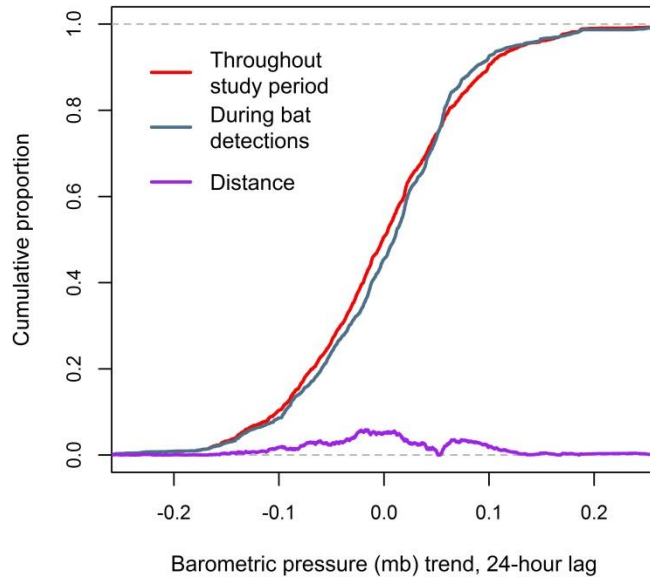


Figure 24. Cumulative distribution functions of barometric pressure trend over a 24-hour lag period during bat detections relative to the monitoring period when no bats were detected. The range of trend values during which bats were more frequently detected span -0.02 to 0.08 corresponding to the beginning of an increase in barometric pressure during the previous night of sampling.

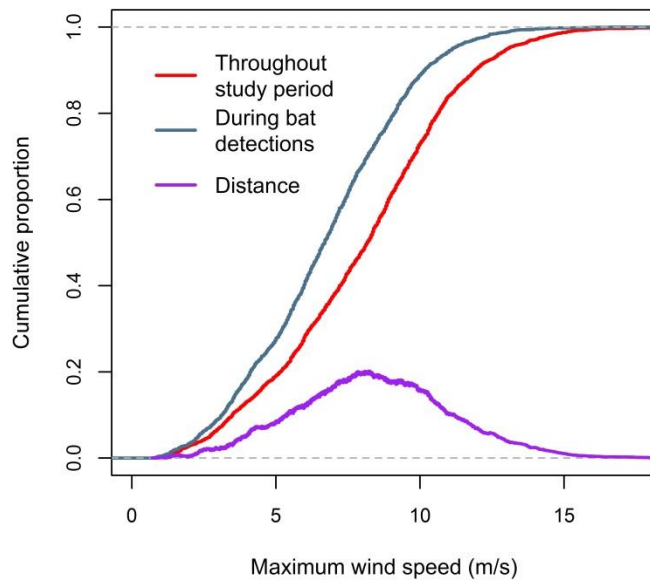


Figure 25. Cumulative distribution functions of maximum wind speed during video detections of bats relative to conditions recorded throughout the monitoring period when no bats were detected. Bats were more likely to be present when maximum wind speeds were < 8.2 m/s.

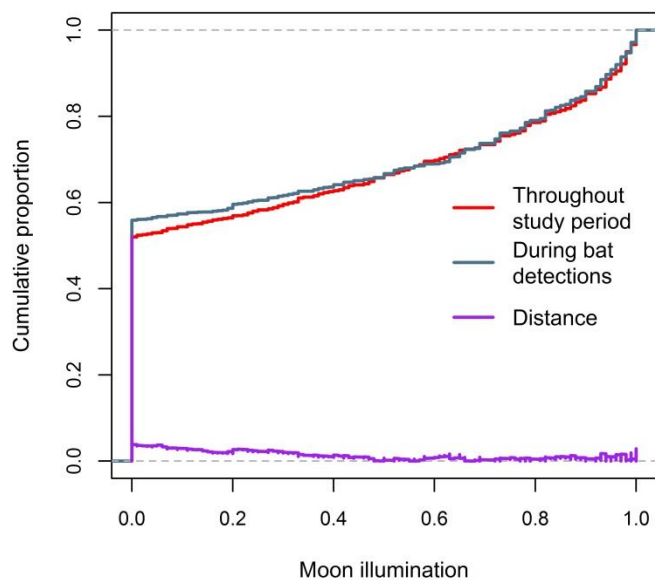


Figure 26. Cumulative distribution functions of moon illumination during video detections of bats relative to illumination recorded throughout the monitoring period when no bats were detected. Illumination was recorded as the proportion of lit lunar disk visible above the horizon. Decreasing distance values indicate relatively less-frequent observations than expected where the function for bat observations occurs above the function for “ambient” conditions. Moon illumination was found to be only marginally related to the frequency of bat detections, with slightly higher activity at low illumination levels.

Patterns of bat activity related to nightly meteorological conditions were examined with regression trees. As with the classification tree analysis of “instantaneous” weather conditions, the analysis found bat detection rates to be negatively associated with gusty, cool, humid and rainy conditions measured over the entire night (Figure 28). The path that favored the highest rates included conditions when nightly maximum wind speeds were ≤ 8.3 m/s and cumulative rain ≤ 0.8 mm. The path that favored the lowest rates included maximum wind speeds > 9.8 m/s, where humidity levels were $> 85.0\%$, and temperatures were ≤ 21.4 °C. Both barometric pressure and mean wind speed were moderately to highly correlated with maximum wind speed ($r = 0.47$ and 0.98 , respectively), and were not identified as significant variables in the model because of collinearity. Preliminary models identified these as significant variables when maximum wind speed was excluded as a potential factor.

The incidence of bat and insect detection appeared to be closely linked both among and within nights. Nightly detections were significantly and positively correlated over the 6-month sampling period ($r = 0.62$; $P < 0.001$), demonstrating similar episodic peaks and dips in the number of insect and bat detections (Figure 29). Hourly rates of detection were also examined between and within nights. Between-night bat and insect detections by hour were significantly correlated when compiled for the entire monitoring period ($r = 0.85$; $P < 0.001$; Figure 30), and the occurrence of insects generally exhibited a bimodal nightly pattern similar to that of bats (see

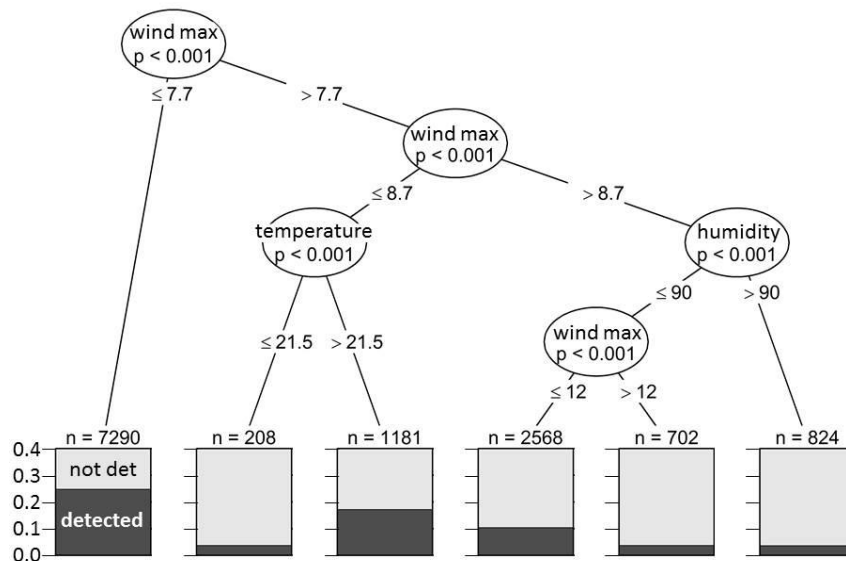


Figure 27. Classification tree model of interactions between weather variables associated with the proportion of bat detections observed by video. The path to the left of each node represents the conditions that lead to higher rates compared with the path to the right of the node. Threshold conditions are indicated by values on the path lines. Bar graphs for each terminal node indicate the proportion of 10-minute intervals with or without a bat detection (“detected” “not det”, respectively) given the conditions represented by that node. The number of 10-minute interval observations (n) associated with each node is specified above each bar graph. For graphical clarity the y-axis was limited to a maximum proportion of 0.4. This model indicates that bat detections was more frequent when maximum wind speeds were ≤ 7.7 m/s. Conversely, a low proportion of detections occurred under a variety of conditions such as when humidity levels were $> 90.0\%$ and maximum wind speeds > 8.7 m/s, or when humidity levels were $\leq 90.0\%$ and maximum wind speeds > 12.0 m/s.

also Figure 12). However, the correlations of hourly detections were more variable when compared individually on a nightly basis. For example, the moderately high correlation of 0.7 for hour 1800 indicated that bats and insects were mostly observed at the same time on the same nights (despite a relatively low number of detections at that hour). In contrast, although the total number of detections was high at hour 2000, the co-occurrence of bats and insects was much less strongly correlated ($r = 0.40$), indicating that bats could be present but insects absent on many nights at that hour (and vice versa). An important caveat to these numbers is that the distance at which bats and insects were imaged by videography differed considerably (insects were detectable only to about 20 m, whereas bats could be detected > 150 m).

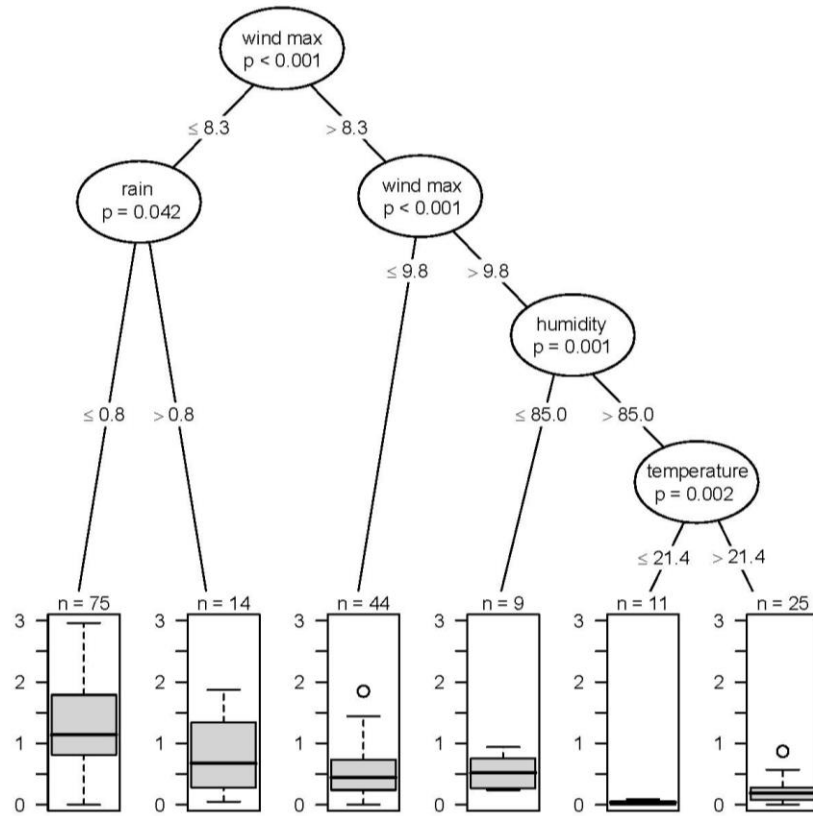


Figure 28. Regression tree model of interactions between weather variables associated with the rate of bat detections observed by video. Detection rate is adjusted by survey effort (i.e., night duration and number of turbines monitored per night). The path to the left of each node represents the conditions that lead to higher rates compared with the path to the right of the node. Threshold conditions are indicated by values on the path lines. Boxplots for each terminal node indicate the nightly bat detection rate given the conditions represented by that node. The significance of the variable is shown below each variable name. The number of nightly observations (n) associated with each node is specified above each bar graph. This model indicates that bat detection rates were highest when nightly maximum wind speeds were ≤ 8.3 m/s and cumulative rain ≤ 0.8 mm, and were lowest when wind speeds were > 9.8 m/s, humidity levels $> 85.0\%$, and temperatures ≤ 21.4 °C.

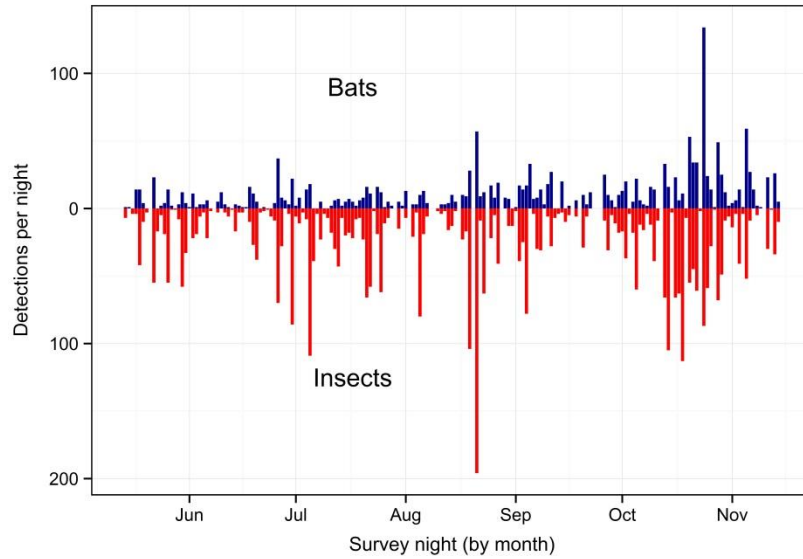


Figure 29. Nightly video detections of bats relative to insect detections at WTG26.

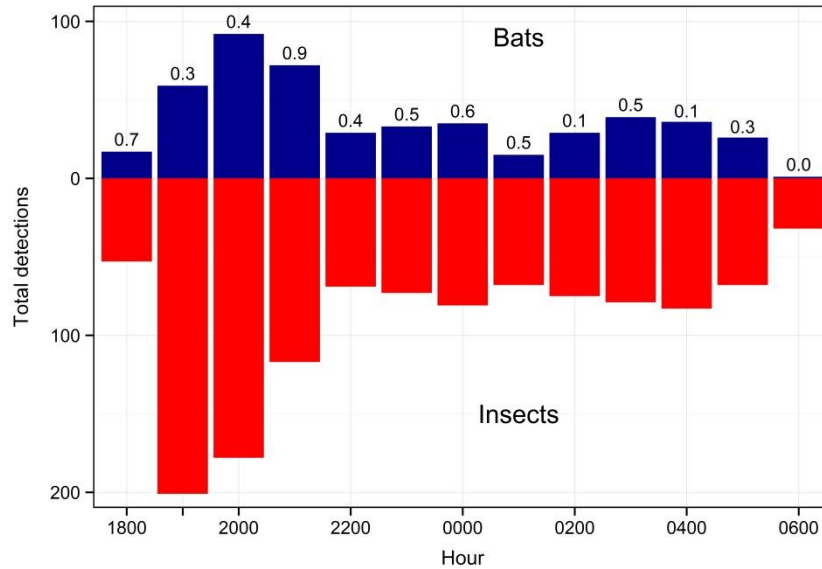


Figure 30. Video detections of bats relative to insect detections. Data depicted are of two types: total detections by hour across all nights (“between-nights”; bars), and hour-to-hour detections by night (“within-nights”; correlation values above bars). Data consist of paired bat-insect samples over the 6-month monitoring period at a single turbine (WTG 26).

The incidence of acoustic bat detections recorded from turbine nacelles were very low compared to the number of video detections. For example, concurrent samples at WTG26 detected bats acoustically on only 8% of the nights sampled, whereas bats were detected by video on 86% of the same nights (Figure 31). Although it is possible that turbine noise or difficulties with operation of acoustic detectors on the turbine nacelles may have contributed to low encounter rates (e.g., high exposure and weathering of microphones), the rates were comparable to those obtained from most ground-based detectors across the study region (see section Occupancy Analysis below).

Terminal phase calls (“feeding buzzes”) were recorded from the nacelle of WTG 26 on only three occasions, and not at all at WTG 23 and 25 during the 6-month monitoring period (WTG 24 had no recordings and may not have been functioning properly). The very low incidence of terminal phase calls may indicate relatively infrequent prey targeting near the nacelle, or be simply an artifact of the generally low emitted intensity and limited detectable range of this type of call (Surlykke & Kalko 2008). For comparison, it is worth noting that terminal phase calls were recorded very infrequently at the ground-based acoustic detectors during the 1-year sampling period (fewer than 5% of the nights sampled at 13 of the 23 sites, and never at the remaining 10 sites.)

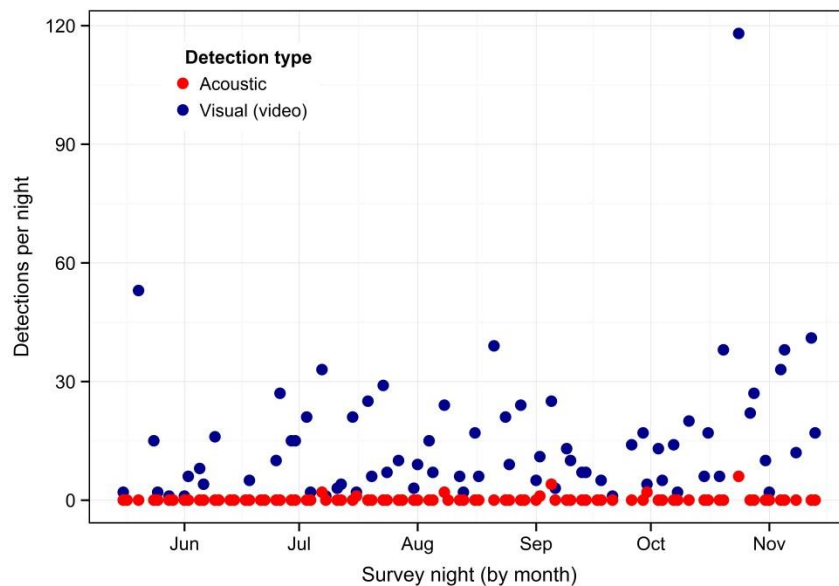


Figure 31. Frequency of acoustic detections on nacelle-mounted bat detectors relative to video detections from ground-based surveillance cameras. For graphical clarity, data are presented for a single turbine (WTG26) on the nights when both sampling methods were operating.

To infer relative bat activity immediately around the nacelle we examined the proportion of acoustic detections recorded from the pair of microphones mounted at the rear and on the bottom of each turbine nacelle (Figure 32). Although the actual shape and overlap of the airspace sampled by the detector microphones is not known, a bat’s location at the time it vocalized was approximated by comparing detections among paired microphones. One-third of

the detections ($n = 27$) were recorded simultaneously in the airspace sampled by both microphones, and indicated that these bats were likely below and to the lee of the nacelle. The majority of detections (57%; $n = 46$) occurred at only the leeward-oriented microphone, and indicated that these bats were located to the rear and possibly above the nacelle. Only a small proportion of detections (10%; $n = 8$) were recorded solely from the microphone oriented directly downward, and indicated that these bats were vocalizing from directly below the nacelle and possibly towards the windward side.

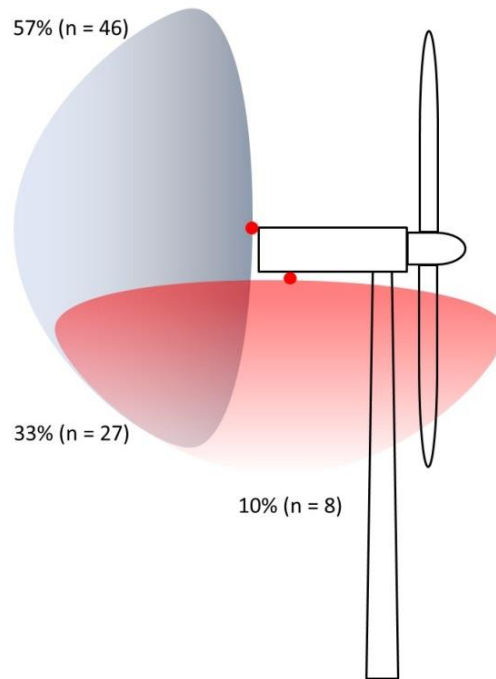


Figure 32. Proportion of acoustic bat detections relative to the hypothetical sampling coverage and overlap of a pair of detector microphones. Red points represent microphone placement. Data are presented for compiled detections from WTG 23, 25 and 26 (WTG 24 had no recordings and may not have been functioning properly).

Bat fatality monitoring

Bias trials

A total of 88 rat carcasses were placed for searcher efficiency and carcass persistence trials. Of the searcher efficiency trials, we had 22 carcasses removed before the first search, which left only 66 carcasses that were available to be found on at least one occasion (Table 3). For carcass removal trials, we were able to use 73 carcasses, and all but one was removed within 20 days.

The model with the lowest AIC_c value for both searcher efficiency and carcass persistence was the “no visibility” class model (Table 3) with the log-logistic being the best-fit distribution for carcass persistence. We estimated average searcher efficiency to be 0.85 (95% CI = 0.76 – 0.92) and average persistence time to be 3.1 days (95% CI = 2.3 – 3.9 days), with an estimated 85% of carcasses (95% CI = 77 – 92%) persisting until the next search.

From these trials we estimated average searcher efficiency to be 0.85 (95% CI = 0.76 – 0.92), although it is important to note that the relatively high range of values may be partly an artifact of the use of rats as surrogates for bat carcasses. The searcher efficiency model with the lowest AIC_c value was the “no visibility” class (Table 4). The carcass persistence model with the lowest AIC_c value was described by a log-logistic distribution in the “no visibility” class.

Table 3. Searcher efficiency and carcass persistence models and AIC_c values, with and without visibility class as a covariate. The selected model within each trial based on lowest AIC_c value is highlighted in bold.

Bias Trial	AIC _c Values	
	Visibility	No Visibility
Searcher Efficiency	59.96	58.21
Carcass Persistence Distribution	Visibility	No Visibility
Weibull	289.55	285.31
Exponential	289.7	285.97
Log-logistic	282.71	279.28
Log-normal	284.2	280.14

Table 4. Top performing models of searcher efficiency and carcass persistence bias trials with surrogate rats at Kawaihoa Wind Power, O’ahu, Hawai’i, 15 May–15 November, 2013. For searcher efficiency, values include number of carcasses placed, number found, and average search efficiency with 95% confidence intervals (CI). For carcass persistence, values include number of carcasses placed, average proportion of carcasses persisting for 1 day (\hat{r}), and estimated average carcass persistence time (\hat{t}_k) with 95% CIs.

Bias Trial			
Searcher Efficiency	Placed 66	Found 56	Mean (95% CI) 0.85 (0.76–0.92)
Carcass Persistence Distribution	Placed	\hat{r} (95% CI)	\hat{t}_k (95% CI)
Log-logistic	73	0.85 (0.77–0.92)	3.07 (2.30–3.87)

Fatality searches

We were able to search turbines 98.4% of the days between 15 May and 15 November, 2013. We were unable to conduct any searches on 23–26 September because of turbine maintenance. Total search time averaged 114 minutes per turbine for an estimated total of 1,383 hours of searching, although there was variation in search times within each turbine plot because of differences between searchers or weather conditions. We found fatalities at WTG 23, 25 and 26, but not at turbine 24. We found six birds and one bat which collectively represented one fatality per 198 search hours. One bird was found 18 m from the turbine base and five were found within 3 m of the turbine base. The bat was found 54 m from the base of WTG 25 at a bearing of 203 degrees. Of the six bird carcasses, we found four Common Myna (*Acridotheres tristis*), one Zebra Dove (*Geopelia striata*), and one Nutmeg Mannikin (*Lonchura punctulata*).

Fatality estimation.

Because too few bats were found to be able to calculate a site-specific density-weighted proportion of bats expected to land within the searched area, we used the approach outlined in Huso and Dalthorp (2014) based on the maximum expected fall distance calculated by Hull and Muir (2010). Using their equation we calculated the maximum distance to be 85.6 m and the density weighted proportion expected to land within a 125 x 120 m plot to be 0.884. Based on the estimated searcher efficiency and carcass persistence described in "Bias Trials" and model parameters described in Appendix 5, the overall detection probability was estimated at was 0.68 (95% CI = 0.62–0.74). Given that there was one observed bat carcass, we estimated that there was less than a 10% chance that total fatality exceeded three bats at the four turbines in our study during the period from May 15 through Nov 15, 2013 (Figure 25, Table 5).

Table 5. Posterior probability distribution that the total fatality (M) at the 4 turbines monitored equals or exceeds a specific number of carcasses (m) given that observed count (X) equaled 1. Values are graphed in Figure 33.

m	Prob(M ≥ m X = 1)
0	1.000
1	1.000
2	0.534
3	0.240
4	0.099
5	0.039
6	0.015
7	0.005
8	0.000

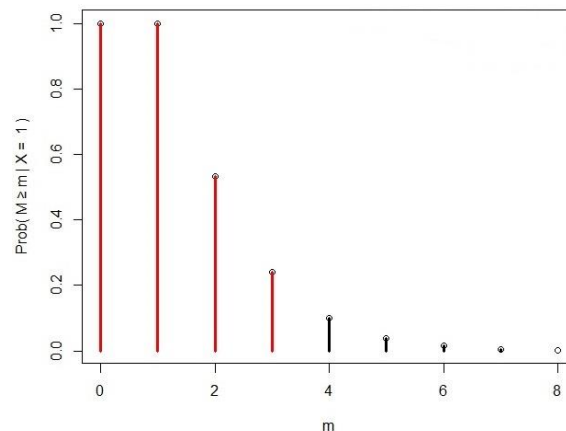


Figure 33. Posterior probability distribution that total fatalities (M) are equal or exceed a specific number (m) given that the total observed carcass count (X) equaled 1. The fatality monitoring results indicate that there was less than 10% probability that total fatalities exceeded 3 bats. Bars that cover less than 10% of distribution are shown as black. Posterior probabilities are presented in Table 5.

DISCUSSION

This study was a unique opportunity to investigate how broader patterns of landscape use by a bat species relate to its presence and behavior at a particular site within the landscape. In this case, the local site was a wind energy facility experiencing fatality of an endangered subspecies, on a Hawaiian island where the distribution and abundance of this endemic bat is poorly understood. To date, there have been few studies relating bat occurrence across broader landscapes to susceptibility at wind turbines. Clear linkages between rates of bat fatality at wind turbines and features of surrounding landscapes have not been found at any spatial scale, with the exception of higher bat fatality rates on forested ridges (Arnett and Baerwald 2013) and perhaps near mountain ranges (Baerwald and Barclay 2009) or shorelines of large water bodies (Heist 2014).

The subfossil record demonstrates that hoary bats arrived in Hawai'i at least 4,800 YBP (Burney et al. 2001) and genetic analysis indicates an initial arrival dating to perhaps as much as 10,000 YBP (Russell et al. In review). Since its arrival *L. cinereus semotus* may have evolved behaviors that differ from its mainland conspecifics. However, our glimpse into the use of broader landscapes around a wind energy facility by this unique, lone island species is still relevant to the general understanding of bat fatalities at wind turbines. In many ways, we believe that the Hawaiian hoary bat is a 'model' species for studying bats and wind turbines by providing a contrast to patterns observed on the mainland by its conspecifics — the bats most frequently and adversely affected by wind turbines.

Our findings indicate that hoary bats were acoustically cryptic and appeared to occur fairly sparsely in the region, with an overall site occupancy rate of 55% over the 1-year period of acoustic monitoring at 23 sites and an 8% chance of acoustically detecting a bat on a given night given that it was present. Although more bats may occur at these sites than were detected acoustically, our findings do not demonstrate high bat abundance in the region. The Hawaiian hoary bat has only once been reported occurring in large numbers on O'ahu, in 1816 (Tomich 1986), and since then observations tend to be infrequent sightings of individual bats (TenBruggencate 2002). Despite this scarcity, we discovered and quantified the first clear links between bat presence and weather and landscape features on O'ahu.

Hawaiian hoary bats were more likely to occur and be acoustically detected in certain parts of the study area than others. Bats were detected less frequently in the windward northern areas than in the leeward southern parts of the study area (which include the wind facility where we monitored local activity by video). In association with this broad pattern, bats were more likely to be detected at higher-elevation sites with flat ridgetops and in areas sheltered from the wind than at lower-elevation sites with rough terrain and more wind. These patterns may be partially attributable to the conditions under which bats are detectable using acoustic devices (e.g., wind and vegetation can influence recording efficiency), but are generally consistent with patterns of activity and distribution (e.g., use of open habitats sheltered from the wind and certain elevation ranges) observed for hoary bats on the Island of Hawai'i (Menard 2001, Gorresen et al. 2013) and with this and other species of bats elsewhere (Barclay 1985, Verboom and Spoelstra 1999, Cryan et al. 2000, Erickson and West 2002). At two of the sites monitored we recorded no activity, despite those bat detectors functioning properly. It is unclear why bats did not apparently occur at these two sites, which were similar to nearby sites. Bats were detected at three of the acoustic monitoring sites more than any others (Figure 4), particularly during the period when detection probability across sites seasonally peaked (Figure 3). These sites may be

avored due to the flatter terrain and wind-sheltered, higher-elevation biotic community they support. Although Hawaiian hoary bats occupied those sites more consistently than others, even there they tended to 'acoustically disappear' from about December through February — somewhat of a surprising finding.

Generally, acoustic detections of Hawaiian hoary bats were consistently low from October through February (e.g., < 10% chance of detecting a bat on a given night at any site monitored) and increased at most sites to peak in April through August (e.g., > 30% chance of nightly detecting bats at the two most-active sites). It is unlikely that physical conditions in the environment change sufficiently during winter to explain this seasonal drop in detection rates. The most likely explanations involve changes in the availability of insect prey, with the result that some or all bats leave the study area during the winter months and/or become much less active while remaining in the study area.

Hoary bats on the Island of Hawai'i are known to move seasonally among island regions and effectively vacate certain habitats during the winter months (Menard 2001, Gorresen et al. 2013). This may also be occurring on O'ahu, but we did not expect such seasonal habitat shifts given the island's smaller size. O'ahu has a land area of 1,559 km² (602 mi²) and a maximum width of 70 km (44 mi), whereas Hawai'i is more than nine times larger in land area (10,414 km² [4,021 mi²]) and more than twice as wide at its farthest-separated shores (149 km [92 mi]). Hoary bats on the mainland have been known to fly up to 70 km in a night (Castle et al. In review), but are generally thought to forage within several km of their roost trees during the period when females are birthing and raising their young (Barclay 1989, Hickey and Fenton 1996, Gorresen et al. 2013). Outside of the reproductive period, hoary bats on the mainland are highly migratory and have evolved a survival strategy in which seasonal continental-scale movement among habitats is the norm (Findley and Jones 1964, Cryan 2003). It is possible that this behavior of seasonal-movement still exists in the population on O'ahu and that they temporarily move to other parts of the island during winter. Year-long occupancy monitoring with acoustic detectors deployed across O'ahu could address this possibility. One possible outcome of such a study could be that the probability of detection and occupancy turns out to be consistently lower across the *entire* island from October through February, and that such decreases are attributable to seasonal changes in the activity of bats.

The winter ecology of hoary bats is still very poorly understood. Despite being one of the most wide-ranging species of bat in the Americas, there have been no detailed studies into exactly where continental hoary bats go during winter, what types of winter roosts they use, and whether most individuals remain active, hibernate, or use an intermediate strategy between these two extremes (Cryan et al. 2014b). Early researchers speculated that most hoary bats occurring in the continental U.S. and Canada move to the warmer parts of Mexico or farther south during winter and remain active (Findley and Jones 1964), but that assumption later came into question as evidence emerged that hoary bats may be present but seasonally inactive in coastal areas of the U.S. (Cryan 2003, Cryan et al. 2014b). Many species of temperate-zone and tropical bats are capable of entering daily torpor when resources are limited or weather conditions are not favorable, and hoary bats are no exception (Genoud 1993, Cryan and Wolf 2003, Geiser and Turbill 2009, Geiser and Stawski 2011). To our knowledge, the populations of hoary bats occurring on the Hawaiian Islands are the only ones in which activity has been consistently detected during months that coincide with temperate-zone winters in the Northern Hemisphere (Menard 2001, Gorresen et al. 2013). Genetic evidence indicates that hoary bats from North America colonized the islands at least twice within about the past 10,000 years, with

the most recent arrival perhaps less than 800 years ago (Russell et al. In review). *Is this sufficient time for Hawaiian hoary bats to lose the highly seasonal behaviors that evolved over tens to hundreds of thousands of years? Although the Hawaiian climate is tropical, might hoary bats on the islands still be responding to the veritable ghost of a Northern Hemisphere temperate-zone winter?* Hoary bats on the Island of Hawai'i move to colder habitats at higher elevations during the winter months and evidence indicates that they are generally less active, presumably due to more frequent use of torpor (Menard 2001, Gorresen et al. 2013). We presumed before this study began that O'ahu did not have enough high-elevation habitats and sufficiently cool temperatures to facilitate torpor in hoary bats on the island. O'ahu only rises 1,231 m (4,040 ft) above sea level and temperatures at higher elevations are less variable than on Hawai'i, where the mountains rise more than three times higher (4,205 m [13,796 ft]) and can have snow in winter. Future studies that use temperature-sensitive radio transmitters could help shed light on the question of whether the winter decline of hoary bat acoustic detections we observed on O'ahu was attributable to winter torpor, or alternatively, greater summer activity.

The seasonal peak in acoustic detections we observed from approximately March through September on O'ahu generally coincides with the period of birth and raising of young hoary bats on Hawai'i and the mainland (Menard 2001, Shump and Shump 1982). Seasonal variability in the timing of birth tends to be lower on the mainland (Shump and Shump 1982), but more variable on the Hawaiian Islands (Tomich 1986), the latter spanning a wider range of months. In a study in Canada, female hoary bats increased their foraging times by at least 73% over the period from when young were born to when young became volant, demonstrating the increased energetic demands imposed by reproduction (Barclay 1989). Female hoary bats are known to reproduce on O'ahu (D. Johnston, H.T. Harvey & Associates, pers. comm.). It is plausible that our observations involving seasonal increases in detection across sites, as well as high rates of detection and occupancy at only a couple of those sites, are attributable to increased activity by reproductive females favoring certain habitats. The seasonal peaks we observed could reflect pregnant and lactating females foraging for longer periods each night in the most productive habitats. Such patterns may predominate if the population is small, such that occupancy trends are more likely to be influenced by the actions of certain individuals in the population. If this were true, then the decreased probability of acoustic detection during December could simply indicate low population numbers and a low baseline level of activity exhibited by bats outside the period of reproduction. The hypothesis of increased activity due to female reproduction, which is testable through capture surveys and radio telemetry but not acoustic methods, might explain the seasonal peak in detections of Hawaiian hoary bats we observed on O'ahu.

There are a number of other possible reasons why acoustic bat detection was very low on O'ahu (especially in comparison to Hawai'i Island). Prey size can influence the range of echolocation frequencies used by bats, and bats may vocalize at higher frequencies to detect relatively small prey if such items predominate (Kingston et al. 2003). However, higher frequencies are more attenuated, particularly in conditions of high humidity, and bats may not be as readily detected at a distance than those using low-frequency calls to target larger prey. The identity of prey species may also be another factor affecting bat detectability. For example, noctuid moths on Kaua'i reveal reduced sensitivity to most frequencies above 25 kHz (Belwood and Fullard 1984), and hoary bats may exploit this by adjusting echolocation frequencies accordingly. Consequently, bat detection may depend to some extent on the prevalence of certain target prey species and their relative size.

Weather generally has a strong influence on bat activity (e.g., Erickson and West 2002). However, on a night-to-night basis the acoustic prevalence of bats across the study region was not obviously associated with changes in weather. This may reflect the fact that these metrics were produced for a 24-hour period (starting at dawn of day 1 and extending to dawn of day 2) that may poorly match the temporal scale of conditions to which bats respond. For example, bats may respond to declining barometric pressure over a period of several days and nights, but immediately respond to rainfall over very short periods (by taking shelter during strong rains and rapidly becoming active once rain has stopped.) In general, bats were detected more often and were more widespread on summer nights with warmer temperatures than on winter nights with cooler temperatures, but the temperature effects were likely partly a correlate of the only other significant association we found for the landscape analyses — Julian date and the seasonal trends discussed above (the correlation of untransformed Julian date and temperature was 0.56). Although our analysis of physical landscape features indicated that bats may occur more often in areas sheltered from the wind, we did not detect an influence of nightly wind speed on the occupancy of sites across the landscape studied. Wind generally blows fairly consistently and steadily across northern O'ahu, so conditions may not have been variable enough for us to detect more subtle effects among the limited number of sites we sampled. Overall, our observations suggest that bats forage under most weather conditions, a capacity also noted for hoary bats on the islands of Kaua'i (Belwood and Fullard 1984) and observed on Hawai'i by several of the authors (PMG, KM, FJB).

Acoustic detectors deployed on the turbines in our study detected bats at similarly low rates to those deployed across the broader landscape. Common assumptions of studies that rely on acoustic detectors to study bats include: 1) the devices consistently detect bats when they are present and calling; 2) the number of calls recorded reflects the number of bats present, or at least relative activity; 3) the number of calls recorded will be similar among similar habitats; 4) the number of calls recorded reflect habitat quality; 5) the number of terminal phase calls (feeding buzzes) detected reflects the amount of feeding occurring at the site; and 6) bats can be reliably identified to species from their echolocation calls (Hayes 2000). Our concurrent observations with video cameras indicated that most of these assumptions were violated in the case of acoustic detectors deployed on wind turbines, with the exceptions of the fourth (quantity reflects quality, an attribute we could not test) and sixth (reliable species identification). We observed multiple instances in which bats flew close to the turbine nacelles and near detector microphones, yet were not recorded (similar to observations at wind turbines in Indiana; Cryan et al. 2014a). We also noted a lack of recorded feeding calls despite concurrent video evidence of frequent foraging-like behavior. In general, our video observations of bats at wind turbines provided a richer source of observations from which to draw inference about conditions influencing occurrence and behaviors of bats near wind turbines.

Technological methods of remotely monitoring wind turbines for rare events such as bat visitation can be tremendously more efficient than human observation in real time. Our findings from thermal surveillance cameras demonstrate the value of remote videographic monitoring. We observed thousands of events involving flying animals over the course of 6 months of monitoring the turbines every night with cameras. Birds were very infrequently observed at night, whereas insects and bats were more common. We recorded over three thousand events involving bats on video (compared to 81 acoustic detections on the four turbines with bat detectors), yet these detections can certainly be considered fairly infrequent events, typically averaging only one or two bat passes per hour. Video surveillance also determined that bat flights near turbines were fairly brief events. The mean duration of a bat pass was about 4

seconds, with a maximum of 360 seconds. Cumulatively, on nights with bat detections these passes totaled to an average of about 42 seconds per night per turbine, with detections in some nights totaling to as much as nine minutes. Overall, bats do not appear to be spending much time at the turbines we monitored. The amount of time during which bats were observed over the 3,847 hours of processed recordings totaled to only about three hours (or about 0.10% of the monitoring time). In other words, surveillance cameras and automated computer processing of the imagery helped us avoid having to sit through the 99.9% of the 6-month monitoring period in which nothing of interest occurred.

Thermal video cameras allow the gathering of more detailed information about the behaviors of bats near wind turbines than other existing monitoring techniques. Thermal cameras were used to observe bat behaviors at turbines in two prior studies. Horn et al. (2008) sampled turbines for 10 nights in West Virginia, USA during autumn of 2004 and among other things observed bats frequently approaching and investigating turbines, chasing slow-moving blades, being struck or displaced by moving blades, regularly foraging in blade-swept areas, and a correlation between insect presence and bat occurrence. Cryan et al. (2014a) used thermal cameras to nightly monitor three experimentally manipulated turbines for approximately two months during late summer and autumn of 2012 at a wind facility in Indiana, USA, and observed bats frequently making close approaches to turbines (typically on the leeward sides), chasing slow-moving blades, being struck or displaced by moving blades, occurring more often at turbines during low wind conditions and on nights with bright moonlight, and rarely flying in ways indicative of foraging near the turbines. In both of these studies, acoustic monitoring or fatalities found on the ground indicated that many of the bats observed were likely species of *Lasiurus* (hoary bats or the closely related eastern red bat, *L. borealis*). These observations from the mainland, where hoary bats are highly migratory and most susceptible to wind turbines during a time of year (mid-July through October) coinciding with autumn migration and mating (Cryan and Brown 2007), provide a backdrop against which to compare and contrast the video observations made during our O'ahu study.

Most video observations made during the six months of turbine monitoring on O'ahu involved a single bat. Less than 3% of events involved more than one bat in the scene and we almost never observed bats chasing or following each other. In the prior study in Indiana, a similar proportion of bats were alone when observed (3% of events were pairs), yet a higher proportion (48%) of the multi-bat events in Indiana involved chasing or following. The vast majority of Hawaiian hoary bats near turbines in the present study made a single pass and only a small proportion of these altered course and closely approached the turbine structure, sometimes repeatedly (*sensu* 'focal behaviors' of Cryan et al. 2014a). In rare instances we also observed Hawaiian hoary bats closely approaching turbine monopoles, nacelles, and closely following slow-moving blades, as was observed more frequently in the prior study. Prevalence of focal behaviors on O'ahu generally was lower (63%; combined "erratic" and "curved" flight) than was observed in the Indiana study (88%), as was the prevalence of multiple approaches during focal events (Cryan et al. 2014a). Video events involving bats at turbines on O'ahu typically lasted only a few seconds, although 10% detections were "sustained", similar to observations from the Indiana study (Cryan et al. 2014a). Considered together, these observations indicate that hoary bats on O'ahu may spend less time near wind turbines and show less interest in them than their more-migratory mainland conspecifics. We speculate that the Hawaiian hoary bats we observed at turbines were local residents going about their daily routine near now-familiar structures within their home range. In contrast, hoary bats observed at wind facilities on the mainland are likely to be approaching and investigating unfamiliar

landscape structures that they might mistake for trees and perceive as a potential resource as they travel long distances (Cryan and Brown 2007, Cryan et al. 2014a). If this is the case, Hawaiian hoary bats may be less susceptible to fatality at wind turbines on a per-encounter basis than hoary bats in continental North America, although different risk factors may be present in Hawai'i.

Video monitoring indicated that the presence of hoary bats near turbines was strongly correlated to insect prevalence. In West Virginia, Horn et al. (2008) observed a correlation between insect and bat presence near wind turbines, as well as peaks in bat activity early in the night and then again toward morning that were comparable to those patterns we observed on O'ahu. Also similar to our study, in which we observed flight indicative of active foraging behavior during 41% of events, Horn et al. (2008) noted that bats "...spend much of their time foraging..." A further indication of close links between bat presence and insects on O'ahu was that the timing of the activity within night did not shift seasonally and that bat and insect detections on video were closely correlated both across nights and within-nights. Bat and insect detections were less closely correlated on an hourly basis and insect numbers were sometimes high without bat presence (and vice versa). In contrast to the findings of the present study and the work of Horn et al. (2008) demonstrating clear evidence of bats feeding near turbines, the observations at turbines in Indiana revealed little evidence of active foraging, although the authors speculated that bats may have been looking for insects at turbines they approached (Cryan et al. 2014a). Findings of the current study offer promise in that they indicate that the presence, and thus risk, of Hawaiian hoary bats at wind turbines may be in part predictable by nightly patterns in the abundance of their insect prey.

Video monitoring shows promise for further investigating links between insect and bat presence at wind turbines. Acoustic detectors mounted on the wind turbines very infrequently recorded bat calls ($n = 81$ events) during the 6-month monitoring period and only three feeding buzz detections typical of foraging, even in instances when video revealed bats engaging in apparent foraging maneuvers within 20 to 30 m of the detector microphones on the nacelle. This low acoustic detection rate, combined with the observation that most calls were recorded from the microphone pointing into the leeward airspace, clearly indicate that acoustic detectors mounted on turbines may chronically under-sample bat activity. The effectiveness of both turbine and ground-level deployment of acoustic detectors has implications for bat monitoring protocols both in Hawai'i and elsewhere. Careful consideration should be given to the duration of sampling efforts and the use of improved acoustic detector devices.

Although the probability of acoustic detection and occupancy of sites by Hawaiian hoary bats were not clearly linked to weather in our broader landscape analysis, video monitoring did reveal several such links at the local scale around turbines. A result consistent to both the "instantaneous" and nightly analyses was that bats were seen near turbines more often than expected during low-wind periods. Several other studies have revealed higher rates of bat activity and fatality around turbines during low-wind conditions (Arnett et al. 2008, Horn et al. 2008, Baerwald et al. 2009, Arnett et al. 2011, Cryan et al. 2014a). In the context of our regional acoustic-based analysis that indicated bats prefer areas sheltered from the wind, as well as our video observations of bats apparently feeding near turbines, it may be that hoary bats are less likely to approach tall structures or find foraging opportunities in the clearings surrounding wind turbines in windy conditions.

Similarly, our observation of higher bat occurrence during times when barometric pressure had fallen over the course of several days, were near or at a low and beginning to climb again indicates that bats may be more likely to approach and forage near turbines when weather conditions are clearing and becoming favorable to aerial insectivores that must capture their prey on the wing. Other authors have suggested that bats, like birds (Breuner et al. 2013), may sense changes in barometric pressure and use pressure changes as a cue in the search for prey (Paige 1995, Turbill 2008).

We observed a negative relationship between humidity and bat occurrence. High-frequency sound attenuates more quickly in humid than in dry air, and humidity directly influences the effective range at which a bat can echolocate (Griffin 1971). The high-frequency calls of bats are therefore less detectable with increasing humidity and acoustic detection bias may partially explain our observations. However, video detections of bats at turbines also declined with increasing humidity and we have no reason to believe that this decline was attributable to camera detection bias. A likely biological explanation for fewer bat detections at high levels of humidity is that foraging by echolocation may be less efficient in wet air. We speculate that Hawaiian hoary bats may not forage as much under high-humidity conditions because of the difficulty of detecting and acquiring insect prey by echolocation in acoustically “denser” air. Simultaneous monitoring with thermal video surveillance cameras and acoustic detectors at variable-humidity sites known to be frequented by foraging hoary bats could help assess this possibility.

Video monitoring revealed a very weak negative relationship between bat presence and moon illumination at the turbines we studied. In contrast, bats were much more likely to be detected at turbines on brightly moonlit nights in Indiana, and it was suggested that those bats may have been visually detecting and orienting toward turbines they mistook for the silhouettes of trees while moving through unfamiliar territory during migration (Cryan et al. 2014a). Combined with our observations of bats seeming to show less-focused interest in the turbines on O’ahu and regularly feeding around them, we speculate that the lack of a strong relationship between moon illumination and bat presence in our study was attributable to familiarity. Unlike the hoary bats in continental North America during autumn migration, bats observed at wind turbines in our study area were more likely to have been local residents in familiar territory. Although these Hawaiian hoary bats may perceive turbines as harboring resources, they may not have the same tendency to closely approach and investigate them (assuming no behaviors of seasonal attraction). If this is the case, bat activity at wind energy facilities in Hawaii may typically involve small numbers of individual bats repeatedly occurring around turbines in their home territory, whereas tens to hundreds of “naïve” hoary bats may pass a turbine on the mainland during autumn migration. These possibilities emphasize the importance of considering assumptions of monitoring and risk-prediction methods, for neither video nor acoustic monitoring are capable of relating the number of detections to the actual number of individual bats present near a turbine. For example, 100 detections by either method could indicate one individual visiting the turbine 100 times or 100 individuals visiting one time each, and thus complicate assessments of risk. Future studies using radio telemetry or other tracking devices could help determine whether hoary bats are seasonally attracted to wind turbines and/or whether the same individuals consistently occur around particular turbines.

Records of bat fatalities at turbines in Hawai‘i indicate that these events occur throughout most of the year (Aaron Nadig, USFWS, pers. comm.). However, despite an intensive effort, only one bat carcass was found at the four turbines during the 6 months of daily searching. The

relatively high overall probability of detection at these turbines (~62–74%) provided strong assurance that this could be interpreted as evidence that few carcasses were likely missed. We can assert that there was less than a 10% chance that total fatality exceeded three bats at the four turbines. In light of the weather and season related patterns of bat activity found in this study, the effect of turbine operation on fatality could be evaluated for experimental treatment. For example, turbine cut-in speed (i.e., wind speed at which turbine blades begin to rotate and wind-generated electricity enters the power grid) could be adjusted during conditions with relatively low versus high periods of bat activity so as to test the effectiveness of operational curtailment on reducing bat fatality at wind turbines.

One of the more puzzling findings of our study was the different peaks in seasonal activity measured by acoustic detectors and by video. As discussed above, acoustic detections show a seasonal peak around May through July, yet our video detection rate more than doubled from May through November. Reasons for these disparate seasonal trends in monitoring data are a mystery, but could be explained by detection bias (e.g., bats less or more detectable by either method in certain seasons) or by actual differences in bat distribution and behaviors around wind turbines compared to other places in the landscapes we sampled. For example, it is hypothesized that during late summer and autumn hoary bats are more likely to visit trees and tree-like structures than during other seasons (Cryan 2014a). If such seasonal behaviors exist, patterns observed at wind turbines on video may be very different from patterns discerned from acoustic detectors not placed in close proximity to structures that concentrate bat activity. In fact, the observation of at least five bats potentially interacting at a turbine over a period of over six minutes on November 14 may indicate a seasonal attraction to emergent structures on the landscape similar to that postulated for the mainland species. Moreover, the trend we observed on video of increasing bat presence near turbines is similar to the trend of increasing fatalities from mid-July onward into October at turbines on the mainland. Video monitoring may be revealing patterns of bat susceptibility to turbines that may not be discernable solely from acoustic monitoring data.

Summary of key study findings

- Video detections of bats occurred throughout the night but were generally bimodal with peaks about 2–3 hours after sunset and four hours before sunrise.
- Bats were detected by video throughout the 6-month monitoring period and demonstrated little evidence of a seasonal shift toward earlier or later night-time activity.
- The hourly rate of nightly bat detection (number/hour/turbine) was highly variable but more than doubled from mid-May to mid-November.
- Almost all video detections were of single bats; < 3% were of multiple bats seen concurrently.
- The duration of most bat video detections were relatively brief and averaged four seconds, although 10% of detections were “sustained” (i.e., lasting \geq 60 seconds).
- The cumulative duration of nightly bat detections averaged 42 seconds, indicating that bats generally did not appear to be spending much time in the rotor-swept zone imaged by video.
- Most (86%) detections involved single bats passing the turbine once, and the largest proportion involved erratic (41%) flight indicative of foraging in the immediate area of the turbine.
- Higher rates of bat detection generally occurred when nightly wind speeds dropped to a low relative to the previous night and mean speeds were < 4.6 m/s and maximum speeds were < 8.2 m/s. Turbines during this study were feathered at wind speeds below 5 m/s and bat behavior may only reflect associated with this curtailment operation.

- Bat detection rates tended to be higher when temperatures were > 22.2 °C, but this may partly reflect the presence of newly volant young in late summer and fall periods rather than the effect of temperature on the activity of individual bats.
- Bats were more likely to occur when barometric pressure was relatively low (≤ 972 mb) but rising over a period of at least 24 hours. Rising barometric pressure may indicate improved conditions for foraging and overall activity and/or increased availability of insect prey; for example, "barometric pressure may be perceived by bats as a cue for predicting the relative abundance of aerial insect prey" (Paige 1995).
- Bat detection was only weakly related to moon illumination; this is in contrast to the findings by Cryan et al. (2014) for a similar study in Indiana.
- Nightly insect and bat detections were significantly and positively correlated, demonstrating a similar bi-modal pattern within-nights and seasonally.
- Bat detection rates acquired by video appear to be only weakly related to nightly averages of weather conditions because the temporal resolution may be too "coarse" and bats can be active during brief intervening periods of otherwise inclement conditions.
- Bats were frequently observed by video flying in close proximity to the turbine nacelle and near detector microphones, yet were not recorded acoustically. This implies that bats may be much less vocal than previously believed, at least at wind turbines and perhaps other tall, emergent structures.
- Despite frequent detections by video of erratic flight indicative of bats foraging, terminal phase calls were very infrequently recorded acoustically and may indicate that bats are not encountering insect prey around the turbine nacelle area.
- Acoustic detections demonstrate a strong seasonal peak not evident in video detections; that is, acoustic detections peak in June and drop steadily through to December, whereas video detections steadily increase from May through November.
- Over half (57%) of acoustic detections at paired microphones were in the area to the rear and above the nacelle, and relatively fewer detections (10%) were directly below and towards the windward side of the nacelle.
- Detection probability across 23 acoustic sample sites was low (mean = 0.08); spatial prevalence of bats was also relatively low (mean = 0.55).
- Acoustic detection probability was generally higher in the leeward (Kawailoa) region compared to the windward (Kahuku) region of the Ko'olau Mountain range.
- Acoustic detection probability was significantly associated with the landscape metrics: elevation (+), topographic position (+) and terrain roughness (-), and wind exposure (-). That is, bats were most frequently detected in generally flatter, sheltered, higher-elevation areas within the study area.
- Prevalence (acoustically) of bats across the region was not strongly associated with weather, and was only significantly correlated with Julian date and temperature (itself partly a correlate of time of year). Nightly averages of weather conditions may be too "coarse" a temporal resolution to use for modeling bat occurrence in some environments.
- The relatively high overall probability of carcass detection provided strong assurance that there was less than a 10% chance that total fatality exceeded three bats at the four turbines during the 6-month period of daily monitoring.

Management implications

It should be noted that these management implications are based primarily on video detections of bats near the rotor-swept zone of four of thirty turbines that were monitored from May–

November 2013. In addition, they assume that higher bat activity is related to higher fatality risk.

- Curtailment strategies for wind turbines intended to reduce bat fatality might be optimized by incorporating weather-related patterns of bat occurrence (in addition to those currently based on average wind speed). For example, turbine cut-in speed (i.e., the wind speed at which wind-generated electricity enters the power grid) could be modified during conditions shown in this study to be associated with higher bat detection rates.
- Barometric pressure emerged in this study as an environmental variable significantly and negatively associated with bat occurrence near turbines. Barometric pressure may be particularly suitable for informing turbine operation in a fatality-reduction context because it exhibited lower hour-to-hour variance than other environmental variables we examined, including wind speed. In this example, cut-in speed could be raised during periods with relatively low and increasing barometric pressure. Note that the observed relationship of bat activity and mean barometric pressure may differ for the period during which video surveillance was not conducted (December to April).
- In addition to weather, turbine operation could be adjusted based on the frequency of bat detections by time of night, such that higher cut-in speeds could be applied during peak bat activity periods, particularly the first third of each night's duration. Because bat detection rates demonstrated little evidence of a seasonal shift toward earlier or later activity as a function of time of night, this curtailment application could potentially be applied consistently throughout the year. However, the duration of video surveillance in this study only spanned a 6-month period (May to November), and these patterns of bat activity should be further investigated with videography for the period between December and April.
- In addition to weather and time of night, turbine operation could potentially be adjusted based on the time of year, with higher cut-in speeds applied during peak bat activity periods from August through November. Bat activity between December and April should be investigated with videography to confirm whether detection rates during this period indeed decline.
- The significant and positive correlation of nightly insect and bat detections warrants further investigation as a relatively simple predictor of bat activity with potential for refining curtailment strategies.
- Given the growing use and reliance of acoustic monitoring to assess relative risk in the proximity of turbines and from turbine nacelles, the low incidence of acoustic detection at turbines should be further investigated and compared to bat detection rates obtained from videographic methods.

ACKNOWLEDGEMENTS

Funding and logistical support for this project was provided by the U.S. Fish and Wildlife Service, the U.S. Geological Survey (Ecosystem Mission) and Bat Conservation International. We thank Mitch Craig and David Cowan of First Wind Energy for giving us the opportunity to do this research at the Kawailoa and Kahuku wind power facilities and for helping with the daily logistics of working at the site. We also thank Matthew Burt of the O'ahu Army Natural Resources Program (Pacific Cooperative Studies Unit at the University of Hawai'i at Mānoa) for facilitating access to the Kawailoa and Kahuku military reservations. We are very grateful to the BCI field crew for their unwavering effort to search for bat carcasses: Sarah Alessi and Kait Lemon. We appreciate the technical assistance provided by Dave Dalton (Bat Research and

Consulting), Paul Fricker (The MathWorks, Inc.), David Hayman (Colorado State University) and Corinna Pinzari (Hawai'i Cooperative Studies Unit [HCSU] at the University of Hawai'i at Hilo). We thank Jim Jacobi (U.S. Geological Survey – Pacific Island Ecosystems Research Center), Todd Mabee (ABR, Inc.), and Julia Rowe (HCSU) for their careful review of this report. Any use of trade, firm, or product names is for descriptive purposes only and does not imply endorsement by the U.S. Government.

LITERATURE CITED

- Arnett, E. B., and E. F. Baerwald. 2013. Impacts of wind energy development on bats: implications for conservation. Pages 435–456 in R. A. Adams and S. C. Pedersen, editors. *Bat evolution, ecology, and conservation*. Springer, New York.
- Arnett, E. B., W. K. Brown, W. P. Erickson, J. K. Fiedler, B. L. Hamilton, T. H. Henry, A. Jain, G. D. Johnson, J. Kerns, R. R. Koford, C. P. Nicholson, T. J. O'Connell, M. D. Piorkowski, and R. D. Tankersley, Jr. 2008. Patterns of bat fatalities at wind energy facilities in North America. *Journal of Wildlife Management* 71:61–78.
- Arnett, E. B., M. M. P. Huso, M. R. Schirmacher, and J. P. Hayes. 2011. Altering turbine speed reduces bat mortality at wind-energy facilities. *Frontiers in Ecology and the Environment* 9:209–214.
- AWS Truewind. 2004. Wind Speed of O'ahu at 50 Meters. http://www.heco.com/vcmcontent/StaticFiles/pdf/HonoluluCounty_Oahu_SPD50m_19July04.pdf.
- Baerwald, E. F., and R. M. R. Barclay. 2009. Geographic variation in activity and fatality of migratory bats at wind energy facilities. *Journal of Mammalogy* 90:1340–1349.
- Baerwald, E. F., J. Edworthy, M. Holder, and R. M. R. Barclay. 2009. A large-scale mitigation experiment to reduce bat fatalities at wind energy facilities. *Journal of Wildlife Management* 73:1077–1081.
- Barclay, R. M. R. 1985. Long-range versus short-range foraging strategies of hoary (*Lasiurus cinereus*) and silver-haired (*Lasionycteris noctivagans*) bats and the consequences for prey selection. *Canadian Journal of Zoology* 63:2507–2515.
- Barclay, R. M. R. 1989. The effect of reproductive condition on the foraging behavior of female hoary bats, *Lasiurus cinereus*. *Behavioral Ecology and Sociobiology* 24:31–37.
- Batschelet, E. 1981. *Circular statistics in biology*. Academic, New York, New York, USA.
- Belwood, J. J., and J. H. Fullard. 1984. Echolocation and foraging behaviour in the Hawaiian hoary bat, *Lasiurus cinereus semotus*. *Canadian Journal of Zoology* 62:2113–2120.
- Braccio, R., and P. Finch. 2011. HCEI Road Map: 2011 Edition (Brochure). No. NREL/SR-7A40-52611. National Renewable Energy Laboratory (NREL), Golden, CO, USA. Last accessed at <http://www.nrel.gov/docs/fy11osti/52611.pdf> on January 25, 2015.
- Breiman, L., J. Friedman, C. J. Stone, and R. A. Olshen. 1984. *Classification and regression trees*. Chapman & Hall, New York.

- Breuner, C. W., R. S. Sprague, S. H. Patterson, and H. A. Woods. 2013. Environment, behavior and physiology: do birds use barometric pressure to predict storms? *The Journal of experimental biology*, 216:1982–1990.
- Boyles, J. G., Cryan, P. M., McCracken, G. F., and Kunz, T. H. 2011. Economic importance of bats in agriculture. *Science*, 332:41–42.
- Burney, D. A., H. F. James, L. P. Burney, S. L. Olson, W. Kikuchi, W. L. Wagner, M. Burney, D. McCloskey, D. Kikuchi, F. V. Grady, R. Gage II, and R. Nishek. 2001. Fossil evidence for a diverse biota from Kaua'i and its transformation since human arrival. *Ecological Monographs* 71:615–641.
- Burnham, K. P. and D. R. Anderson. 2002. *Model selection and inference: a practical information-theoretic approach*. New York, Springer.
- Castle, K. T., T. J. Weller, P. M. Cryan, C. D. Hein, and M. D. Schirmacher. In review. A novel suturing technique for attaching miniature GPS and data logger tags to study broad-scale movements of insectivorous bats.
- Cryan, P., M. Bogan, and J. Altenbach. 2000. Effect of elevation on distribution of female bats in the Black Hills, South Dakota. *Journal of Mammalogy* 81:719–725.
- Cryan, P. M. 2003. Seasonal distribution of migratory tree bats (*Lasiurus* and *Lasionycteris*) in North America. *Journal of Mammalogy* 84:579–593.
- Cryan, P. M., and A. C. Brown. 2007. Migration of bats past a remote island offers clues toward the problem of bat fatalities at wind turbines. *Biological Conservation* 139:1–11.
- Cryan, P. M., P. M. Gorresen, C. D. Hein, M. R. Schirmacher, R. Diehl, M. Huso, D. T. S. Hayman, P. Fricker, F. Bonaccorso, D. H. Johnson, K. Heist, and D. Dalton. 2014a. Behavior of bats at wind turbines. *Proceedings of the National Academy of Sciences* 111:15126–15131.
- Cryan, P. M., C. A. Stricker, and M. B. Wunder. 2014b. Continental-scale, seasonal movements of a heterothermic migratory tree bat. *Ecological Applications* 24:602–616.
- Cryan, P. M., and B. O. Wolf. 2003. Sex differences in the thermoregulation and evaporative water loss of a heterothermic bat, *Lasiurus cinereus*, during its spring migration. *Journal of Experimental Biology* 206:3381–3390.
- Dalthorp, D. H., M. M. P. Huso, D. Dail, and J. Kenyon. 2014. Evidence of Absence Software, USGS Data Series 881. USGS, Corvallis, OR.
- De La Cueva Salcedo, H., M. B. Fenton, M. B. C. Hickey, and R. W. Blake. 1995. Energetic consequences of flight speeds of foraging red and hoary bats (*Lasiurus borealis* and *Lasiurus cinereus*; Chiroptera: Vespertilionidae). *Journal of Experimental Biology* 198:2245–2251.
- De Reu, J., J. Bourgeois, M. Bats, A. Zwertvaegher, V. Gelorini, P. De Smedt, W. Chu, M. Antrop, P. De Maeyer, P. Finke, M. Van Meirvenne, J. Verniers, and P. Crombé. 2013. Application of the topographic position index to heterogeneous landscapes. *Geomorphology* 186:39–49.

- ESRI (Environmental Systems Research Institute). 2014. ARCGIS 10 SP3, Redlands, CA.
- Erickson, J., and S. West. 2002. The influence of regional climate and nightly weather conditions on activity patterns of insectivorous bats. *Acta Chiropterologica* 4:17–24.
- Findley, J. S., and C. Jones. 1964. Seasonal distribution of the hoary bat. *Journal of Mammalogy* 45:461–470.
- Geiser, F., and C. Stawski. 2011. Hibernation and torpor in tropical and subtropical bats in relation to energetics, extinctions, and the evolution of endothermy. *Integrative and Comparative Biology* 51:337–348.
- Geiser, F., and C. Turbill. 2009. Hibernation and daily torpor minimize mammalian extinctions. *Naturewissenschaften* 96:1235–1240.
- Genoud, M. 1993. Temperature regulation in subtropical tree bats. *Comparative Biochemistry and Physiology* 104A:321–331.
- Giambelluca, T. W., Q. Chen, A. G. Frazier, J. P. Price, Y. -L. Chen, P. -S. Chu, J. K. Eischeid, and D. M. Delparte. 2013. Online Rainfall Atlas of Hawai'i. *Bull. Amer. Meteor. Soc.* 94:313–316. <http://rainfall.geography.hawaii.edu/rainfall.html>.
- Gorresen, P. M., A. C. Miles, C. M. Todd, F. J. Bonaccorso, and T. J. Weller. 2008. Assessing bat detectability and occupancy with multiple automated echolocation detectors. *Journal of Mammalogy*, 89:11–17
- Gorresen, P. M., F. J. Bonaccorso, C. A. Pinzari, C. M. Todd, K. Montoya-Aiona, and K. Brinck. 2013. A Five-year study of Hawaiian Hoary Bat (*Lasiurus cinereus semotus*) occupancy on the Island of Hawai'i. Hawaii Cooperative Studies Unit, University of Hawaii at Hilo, Technical Report 41:1–48.
- Griffin, D. R. 1958. *Listening in the dark: the acoustic orientation of bats and men*. Yale University Press, New Haven, Connecticut, U.S.A.
- Griffin, D. R. 1971. The importance of atmospheric attenuation for the echolocation of bats (Chiroptera). *Animal Behaviour* 19:55–61.
- Hayes, J. P. 2000. Assumptions and practical considerations in the design and interpretation of echolocation-monitoring studies. *Acta Chiropterologica* 2:225–236.
- Heist, K. 2014. *Assessing bat and bird fatality risk at wind farm sites using acoustic detectors*. University of Minnesota, Saint Paul, MN.
- Hickey, M. B. C., and M. B. Fenton. 1996. Behavioural and thermoregulatory responses of female hoary bats, *Lasiurus cinereus* (Chiroptera: Vespertilionidae), to variations in prey availability. *Ecoscience* 3:414–422.
- Hope, G. M., and K. P. Bhatnagar. 1979. Electrical response of bat retina to spectral stimulation: comparison of four microchiropteran species. *Experientia* 35:1189–1190.
- Horn, J. W., E. B. Arnett, and T. H. Kunz. 2008. Behavioral responses of bats to working wind turbines. *Journal of Wildlife Management* 72:123–132.

- Hothorn, T., K. Hornik, C. Strobl, and A. Zeileis. 2011. Party: a laboratory for recursive partitioning version 1.0. (<http://cran.r-project.org/web/packages/party/index.html>).Hull, C., and S. Muir. 2010. Search areas for monitoring bird and bat carcasses at wind farms using a Monte-Carlo model. *Australian Journal of Environmental Management* 17:77–87.
- Hull, C. L., and S. Muir. 2010. Search areas for monitoring bird and bat carcasses at wind farms using a Monte-Carlo model. *Australasian Journal of Environmental Management* 17:77–87.
- Huso, M. M. P., and D. H. Dalthorp. 2014. Accounting for unsearched areas in estimating wind turbine-caused fatality. *Journal of Wildlife Management* 78:347–358.
- Huso, M. M. P., N. Som, and L. Ladd. 2012. Version 1.0 Computer Program, Fatality Estimator Software, USGS Data Series 729. USGS, Corvallis, OR.
- Huso, M. M. P., D. Dalthorp, L. Madsen, and D. Dail. In press. Estimating turbine-caused bird and bat fatality when zero carcasses are observed. *Ecological Applications* <http://dx.doi.org/10.1890/14-0764.1>.
- Kingston, T., G. Jones, Z. Akbar, and T. H. Kunz. 2003. Alternation of echolocation calls in 5 species of aerial-feeding insectivorous bats from Malaysia. *Journal of Mammalogy* 84:205–215.
- Korner-Nievergelt, F., P. Korner-Nievergelt, O. Behr, I. Niermann, R. Brinkmann, and B. Hellriegel. 2011. A new method to determine bird and bat fatality at wind energy turbines from carcass searches. *Wildlife Biology* 17:350–363.
- Korner-Nievergelt, F., I. Niermann, O. Behr, R. Brinkmann, P. Korner, B. Hellriegel, and M. M. Huso. 2012. Version 1.0 Computer Program, Estimation of the number of fatalities from carcass searches, R package.
- Kunz, T. H., E. B. Arnett, W. P. Erickson, A. R. Hoar, G. D. Johnson, R. P. Larkin, M. D. Strickland, R. W. Thresher, and M. D. Tuttle. 2007. Ecological impacts of wind energy development on bats: questions, research needs, and hypotheses. *Frontiers in Ecology and the Environment* 5:315–324.
- Lin, M., H. C. Lucas Jr, and G. Shmueli. 2013. Too big to fail: large samples and the p-value problem. *Information Systems Research* 24:906–917.
- Logan, D. M., 2011. *Biostatistical design and analysis using R: a practical guide*. Wiley-Blackwell, Chichester, UK.
- MacKenzie, D. I., J. D. Nichols, G. D. Lachman, S. Droege, J. A. Royle, and C. A. Langtimm. 2002. Estimating site occupancy rates when detection probabilities are less than one. *Ecology* 83:2248–2255.
- Mazerolle, M. J. 2015. Package AICcmodavg. <http://cran.r-project.org/web/packages/AICcmodavg/index.html>
- Menard, T. 2001. Activity patterns of the Hawaiian hoary bat (*Lasiurus cinereus semotus*) in relation to reproductive time periods. M.S. Thesis. University of Hawai'i, Honolulu.

- Mistry, S., and G. F. McCracken. 1990. Behavioural response of the Mexican free-tailed bat, *Tadarida brasiliensis*, to visible and infra-red light. *Animal Behaviour* 39:598–599.
- NOAA. 2002. Climatography of the United States No. 81—monthly station normals of temperature, precipitation, and heating and cooling degree days, 1971–2000. National Oceanic and Atmospheric Administration National Climatic Data Center, Asheville. http://www.ncdc.noaa.gov/climate_normals/clim81/HInorm.pdf.
- Olden, J. D., J. J. Lawler, and N. LeRoy-Poff. 2008. Machine learning methods without tears: a primer for ecologists. *Q. Rev. Biol.* 83:171–193.
- Paige, K. N. 1995. Bats and barometric pressure: conserving limited energy and tracking insects from the roost. *Functional Ecology* 9:463–467.
- R Development Core Team. 2011. R: a language and environment for statistical computing. R Foundation for Statistical Computing, Vienna, Austria. <http://www.r-project.org>.
- Riley, S. J., S. D. DeGloria, and R. Elliot. 1999. A terrain ruggedness index that quantifies topographic heterogeneity. *Intermountain Journal of Sciences* 5:23–27.
- Rodhouse, T. J., K. T. Vierling, and K. M. Irvine. 2011. A practical sampling design for acoustic surveys of bats. *Journal of Wildlife Management* 75:1094–1102.
- Russell, A. L., C. A. Pinzari, M. J. Vonhof, K. J. Olival, F. J. Bonaccorso. (In review). Two tickets to paradise: multiple dispersal events in the founding of hoary bat populations in Hawai'i. *PLoS ONE*.
- Shump, K. A., and A. U. Shump. 1982. *Lasiurus cinereus*. *Mammalian Species* 185:1–5.
- Stolwijk, A. M., H. Straatman, and G. A. Zielhuis. 1999. Studying seasonality by using sine and cosine functions in regression analysis. *Journal of Epidemiology and Community Health* 53:235–238.
- Surlykke, A., and E. K. V. Kalko. 2008. Echolocating bats cry out loud to detect their prey. *PLoS ONE* 3:e2036.
- SWCA (Environmental Consultants). 2010. Kahuku Wind Power Habitat Conservation Plan. Prepared for Kahuku Wind Power LLC.
- SWCA (Environmental Consultants). 2011. Kawaihoa Wind Power Draft Habitat Conservation Plan. Prepared for Kawaihoa Wind Power LLC.
- Szumilas, M. 2010. Explaining odds ratios. *Journal of the Canadian Academy of Child and Adolescent Psychiatry* 19:227–229.
- TenBruggencate, J. 2002. Bat stages rare show on O'ahu. *The Honolulu Advisor*, Honolulu, HI.
- Tomich, P. Q. 1986. *Mammals in Hawai'i*, 2nd Edition. Bishop Museum Press, Honolulu.
- Turbill, C. 2008. Winter activity of Australian tree-roosting bats: influence of temperature and climatic patterns. *Journal of Zoology* 276:285–290.

- Verboom, B., and K. Spoelstra. 1999. Effects of food abundance and wind on the use of tree lines by an insectivorous bat, *Pipistrellus pipistrellus*. *Canadian Journal of Zoology* 77:1393–1401.
- Warren-Hicks, W., J. Newman, R. Wolpert, B. Karas, and L. Tran. 2013. Improving methods for estimating fatality of birds and bats at wind energy facilities. California Wind Energy Association, Berkely, CA.
- Weller, T. J., and J. A. Baldwin. 2012. Using echolocation monitoring to model bat occupancy and inform mitigations at wind energy facilities. *The Journal of Wildlife Management* 76:619–631.

APPENDIX 1. MATLAB CODE USED FOR FINDING BATS AND OTHER TARGETS IN THERMAL SURVEILLANCE CAMERA FOOTAGE

These processing steps require MATLAB and the MATLAB Image Processing Toolbox

The code was designed to analyze 3-channel, false-color digital imagery recorded using the "Ice-and-Fire" color setting on the Axis Q1922-E thermal surveillance camera. It will need to be modified to analyze any other type of video imagery.

Axis Q1922-E cameras programmed to export video files using the H.264 video codec will save exported files in Advanced Systems Format (ASF or .asf). Prior to analysis in MATLAB, these ASF files must be converted to AVI format.

The free program VirtualDub (virtualdub.org) is a quick and efficient way to batch convert .asf files into usable .avi format. In VirtualDub, set the Video control to "Direct Stream Copy", open the file to be converted (it will take a short time to be indexed), type Ctrl+Shift+F7 to "Save as AVI" in batch mode, repeat for all files to be converted, then type F4 to view Job Control panel and "Start" batch processing.

For this analysis we used 64-bit versions of the x264vfw (<http://en.wikipedia.org/wiki/X264>) or ffdshow (<http://en.wikipedia.org/wiki/Ffdshow>) video codecs (if viewOutputs code below results in some frames showing red circles in wrong places, install ffdshow codec after x264vfw and analyze video results on same computer with which the imagery was processed).

This code works well with background sky conditions ranging from clear and uniform through moderate passage of slow-moving clouds or overcast conditions. Low and fast moving clouds still cause considerable numbers of false-positive detections, sometimes numbering in the thousands per night of imagery. We erred on the side of caution and manually reviewed these false positives rather than risk missing events involving bats during cloudy conditions.

Synopsis of the software.

File	Type	Purpose	Calls
batchProcessAVIFiles.m	script	Batch processing a set of video files (AVI). Main entry point for the code.	runAnalysisBatch
runAnalysisBatch.m	function	Process all the specified frames in a given AVI-file.	
isSkyClear.m	function	Determine whether frames will be processed with processFrameClear or processFrameCloudy.	runAnalysisBatch
processFrameClear.m	function	Process a series of frames if sky is clear.	isSkyClear
processFrameCloudy.m	function	Process a series of frames if sky is cloudy.	isSkyClear
showBats.m	function	Generate a display of an individual video frame,	processFrameClear or processFrameCloudy

		highlighting the location of any identified object.	
viewOutputs.m	script	Generate a display showing the number of targets detected in an entire video file, and images of the frames in which objects were detected.	showBats

```
% MATLAB code for batch processing all video files in Audio Video Interleave
% (AVI or .avi) format in a given folder. This is the only code that needs
% to be started in MATLAB to process the video files (but see function
% viewOutputs below for reviewing results).
```

```
% batchProcessAVIFiles
```

```
% Specify the file path and name of folder containing the .avi files
% you want to process:
```

```
data_folder = 'C:\EXAMPLEFOLDER';
```

```
% Read the contents of the folder and identify the AVI-files:
```

```
% -----
data_files = dir(data_folder);
data_files = {data_files.name}; % All files in the folder
[~,ext] = strtok(data_files, '.'); % Get the extensions for each file
is_avi = strcmp(ext, '.avi'); % Identify which extensions are "AVI"
avi_files = data_files(is_avi); % Select only the AVI-files
avi_file_names = the_names(is_avi); % Get file names without extension
```

```
% Build a list of output file names, based on the input names:
```

```
% -----
output_files = strcat('output_',avi_file_names, '.mat');
```

```
% Execute the batch processing of the files:
```

```
% -----
for k = 1:length(avi_files)
    runAnalysisBatch(fullfile(data_folder,avi_files{k}), ...
                    fullfile(data_folder,output_files{k}))
end
```

```
% Processing results will appear in the specified folder as they are
% generated and will have a .mat suffix
```

```
% MATLAB code for running the analysis (automatically invoked by function
% batchProcessAVIfiles)
```

```
function runAnalysisBatch(input_file, output_file)
```

```
% Create a VideoReader object to connect to the file:
```

```
% -----
obj = VideoReader(input_file);
```

```

% Read the first frame (make sure the connection is good):
% -----
f = obj.read(1); %#ok<NASGU>

% Initialize the required variables:
% -----
N_frames = get(obj, 'NumberOfFrames');
idx = 1:N_frames; % All frames
is_bat = false(length(idx),1);

% Execute the processing:
% -----
for k = 1:30:length(idx) % The value between the two colons sets the frame
processing interval, in this case every 30 frames
    is_bat(k) = processFrame(obj,idx(k));

    if mod(k,100)==0 % Save the data after every 100 frames
        save(output_file,'is_bat','idx')
    end
end
save(output_file,'is_bat','idx') % Save the data one last time

```

```

% MATLAB code to determine whether any clouds are present in a video frame.
%(automatically invoked by function runAnalysisBatch)

function tf = isSkyClear(f)

% Remove the black banner at the top of the video frame:
% -----
f = f(25:end, :, :);

% Identify the pixels which correspond to the turbine:
% -----
is_turbine = f(:, :, 1) > 150; % Red channel; original code
is_turbine = f(:, :, 1) > 200 | f(:, :, 3) < 70; % Alternative code; red and blue
is_turbine = bwareaopen(is_turbine, 30000); % Remove relatively small objects
is_turbine = imfill(is_turbine, 'holes'); % Cleanup
is_turbine = imdilate(is_turbine, strel('disk', 10)); % Expand the turbine a
little bit; originally set at 5

% Identify the pixels which correspond to sky:
% -----
is_sky = f(:, :, 1) < 150 & f(:, :, 3) > 100; % Red and Blue channels
is_sky = f(:, :, 1) < 100 & f(:, :, 3) > 200; % Red and Blue channels
is_sky = f(:, :, 1) < 100 & f(:, :, 2) < 100 & f(:, :, 3) > 180; % Red and Blue
channels

% Identify the pixels which correspond to cloud:
% -----
is_cloud = ~is_sky & ~is_turbine; % Whatever is in between the turbine and
sky corresponds to cloud
n_cloud(1) = sum(is_cloud(:)); % Count the remaining red (cloud) pixels
n_not_cloud(1) = sum(is_sky(:)); % Count the remaining red (not cloud)
pixels

```

```

tally = n_cloud(1)/n_not_cloud(1)

% Output: Is any cloud present:
tf = all(n_cloud/n_not_cloud < 0.04); % Adjust threshold as needed
% sets the threshold for the maximum proportion of is_cloud pixels
% in a frame relative to is_sky;
% if above threshold frame goes to processFrameCloudy



---



% MATLAB code for processing video frames with clear sky to remove turbine
% and identify remaining moving objects (automatically invoked by function
% runAnalysisBatch)

function [is_bat,locations] = processFrameClear(obj,idx)
% Process a frame of video to identify whether a bat is present.
% Clear sky case.

% Read a frame from the video file:
% -----
f = obj.read(idx);

% Specify which segmentation method to use:
% -----
method = 1; % This method handles non-uniform sky better
switch method
    case 1
        is_turbine = f(:,:,3)<150;
    case 2
        is_turbine = f(:,:,1)<10 | f(:,:,3)<150;
    case 3
        is_turbine = f(:,:,2)<60 & f(:,:,3)<150;
    case 4
        is_turbine = f(:,:,1)<40 | ...
                    f(:,:,2)<220 | ...
                    f(:,:,3)<200;
    otherwise
end

% Specify the size of the disk structure element to use in the
% dilation/erosion of the segmented objects:
% -----
se_size = 8;

% Oversize the data to avoid dilating the objects to the edges:
% -----
is_turbine = [is_turbine(1,1)*ones(se_size) repmat(is_turbine(1,:),se_size,1)
is_turbine(1,end)*ones(se_size)
            repmat(is_turbine(:,1),1,se_size) is_turbine
repmat(is_turbine(:,end),1,se_size)
            is_turbine(end,1)*ones(se_size)
repmat(is_turbine(end,:),se_size,1) is_turbine(end,end)*ones(se_size)];

% Perform the dilation/erosion, in order to (hopefully) capture spurious
% objects at the edges of the turbine blades:
% -----
se = strel('disk',se_size);

```

```

is_turbine = imclose(is_turbine,se);
is_not_turbine = imclearborder(is_turbine);

% Eliminate the edge padding introduced earlier:
% -----
is_not_turbine = is_not_turbine(se_size+1:end-se_size, ...
                               se_size+1:end-se_size);

% Determine whether a bat is present in the frame:
% -----
is_bat = any(is_not_turbine(:));

% If requested, return the position(s) of the bat(s):
% -----
if nargin==2
    if is_bat
        stats = regionprops(is_not_turbine,'Centroid');
        locations = vertcat(stats.Centroid);
    else
        locations = [];
    end
end

% [EOF] processFrameClear

```

```

% MATLAB code for processing video frames with cloudy sky to remove turbine
% and identify remaining moving objects (automatically invoked by function
% runAnalysisBatch)

```

```

function [is_bat,locations] = processFrameCloudy(obj,idx)
% Cloudy sky case.
% 02/28/2014

```

```

% Input checking:
% -----
N_frames = get(obj,'NumberOfFrames');
if idx > N_frames-1
    is_bat = false;
    locations = [];

    return
end

```

```

% Read the next frame:
% -----
f0 = obj.read(idx);
f1 = obj.read(idx+1);

```

```

% Find the turbine in both frames:
% -----
is_turbine0 = f0(:,:,1)>200 | f0(:,:,3)<70;
is_turbine0 = bwareaopen(is_turbine0,30);
is_turbine1 = f1(:,:,1)>200 | f1(:,:,3)<70;
is_turbine1 = bwareaopen(is_turbine1,30);
is_turbine = imdilate(is_turbine0 | is_turbine1,strel('disk',25));

```

```

is_cloud = f0(:,:,1)<10 & f0(:,:,2)<10 & f0(:,:,3)>200 | ...
           f1(:,:,1)<10 & f1(:,:,2)<10 & f1(:,:,3)>200 ;
is_cloud = bwareaopen(is_cloud,5);
is_cloud = imdilate(is_cloud,strel('disk',5));
is_turbine = is_turbine | is_cloud;

% Find the difference between the previous and current frame:
% -----
d = imabsdiff(f1,f0);

% Find identifiable changes between the frames and clean them up:
% -----
p = ( d(:,:,1)>20 & d(:,:,2)>40 & d(:,:,3)>50 ); % Adjust red, green blue
settings as needed

p = bwareaopen(p,5); % Remove remaining small objects
p = imclose(p,strel('disk',5)); % Merge smaller objects with nearby larger
ones

% Combine with the turbine body, to amalgamate small objects near the
% blades into the blades, and then remove the turbine body:
% -----
r = p;
r(is_turbine | is_cloud) = false;

% Set minimum and maximum RGB color thresholds of target
% -----
min_colors = [0 0 0];
max_colors = [60 50 200];

% Remove objects outside a specified size range:
% -----
size_limits = [2 150]; % Allowed sizes in pixels
r = bwareaopen(r,size_limits(1)) & ...
    ~bwareaopen(r,size_limits(2));

[~,N] = bwlabel(r);

if N==0
    is_bat = false;
    locations = [];
elseif N==1 % One object found
    stats = regionprops(r,d(:,:,1),'Centroid');
    ch1 = regionprops(r,d(:,:,1),'PixelValues');
    ch2 = regionprops(r,d(:,:,2),'PixelValues');
    ch3 = regionprops(r,d(:,:,3),'PixelValues');

    % Check whether the pixel values correspond to a target
    if any( ch1.PixelValues >= min_colors(1) & ...
           ch1.PixelValues <= max_colors(1) ) && ...
       any( ch2.PixelValues >= min_colors(2) & ...
           ch2.PixelValues <= max_colors(2) ) && ...
       any( ch3.PixelValues >= min_colors(3) & ...
           ch3.PixelValues <= max_colors(3) )

        is_bat = true;
        locations = stats.Centroid;

```



```

else
    is_bat    = false;
    locations = [];
end

elseif N==2 % Two objects found
    stats =
regionprops(r,d(:,:,1),'Area','Centroid','PixelValues','MajorAxisLength');
    areas      = [stats.Area];
    bat_length = max([stats.MajorAxisLength]);
    displacement = stats(1).Centroid - stats(2).Centroid;
    displacement = norm(displacement);

% To make sure the two objects could be a bat in two consecutive
% frames, check the distance between the objects.
if any(displacement < 5*bat_length)
    ch1 = regionprops(r,d(:,:,1),'PixelValues');
    ch2 = regionprops(r,d(:,:,2),'PixelValues');
    ch3 = regionprops(r,d(:,:,3),'PixelValues');

% Loop through the objects to determine whether they are bats
% based on their color properties.
for k = 1:N
    if any( ch1(k).PixelValues >= min_colors(1) & ...
           ch1(k).PixelValues <= max_colors(1) ) && ...
       any( ch2(k).PixelValues >= min_colors(2) & ...
           ch2(k).PixelValues <= max_colors(2) ) && ...
       any( ch3(k).PixelValues >= min_colors(3) & ...
           ch3(k).PixelValues <= max_colors(3) )

        is_bat(k)          = true; %#ok<AGROW>
        centroid(k).location = stats(k).Centroid; %#ok<AGROW>
    else
        is_bat(k)          = false; %#ok<AGROW>
        centroid(k).location = []; %#ok<AGROW>
    end
end

if all(is_bat) % Both objects are bats
    is_bat    = true;
    locations = centroid(areas == max(areas)).location;
elseif all(~is_bat) %neither object is a bat
    is_bat    = false;
    locations = [];
else % One of the two objects is a bat
    locations = centroid(is_bat).location;
    is_bat    = true;
end

else % The objects are too far apart to be a bat in two consecutive
frames.
    is_bat    = false;
    locations = [];
end

elseif N>2 % More than two objects were found, meaning some must be false
positives.
    stats = regionprops(r,'Area','Centroid');
    % Filter the objects further, based on size (area)

```

```

    if ~isempty(stats)
        areas = [stats.Area];
        size_differences = abs(areas-mean(size_limits));
        is_best_size = size_differences==min(size_differences);
        idx_best_size = find(is_best_size,1,'first');

        is_bat = true;
        locations = stats(idx_best_size).Centroid;
    else % No objects were found within the size limits
        is_bat = false;
        locations = [];
    end

end

% [EOF] processFrameCloudy

-----

% MATLAB code for generating spatial locations of identified objects for
% visualization (automatically invoked by function viewOutputs [below])

function showBats(obj,idx)

% Display a frame of video, with any bats present
%-----

f = obj.read(idx);

if isSkyClear(f)
    showBatsClear(obj,idx)
else
    showBatsCloudy(obj,idx)
end

% [EOF] showBats

%-----
function showBatsClear(obj,idx)

[is_bat,locations] = processFrameClear(obj,idx);

f = obj.read(idx);
imshow(f,'Border','tight')
if any(is_bat)
    hold on
    plot(locations(:,1),locations(:,2),'or','MarkerSize',20,'Linewidth',3)
    hold off
end

% [EOF] showBatsClear

%-----
function showBatsCloudy(obj,idx)

[is_bat,locations] = processFrameCloudy(obj,idx);

```

```

f = obj.read(idx);
imshow(f,'Border','tight')
if any(is_bat)
    hold on
    plot(locations(:,1),locations(:,2),'or','MarkerSize',20,'Linewidth',3)
    hold off
end

% [EOF] showBatsCloudy

```

```

% MATLAB code for displaying a Figure with the number of targets detected
% in the entire video sequence followed by sequential Figures of frames in
% which objects were identified, with identified objects circled in red.
% Pressing any computer key advances the Figure sequence.

```

```

% Prior to reviewing files, be sure to set the file path in MATLAB to the
% folder containing the video file and associated output.mat results file.
% Also be sure to "CLEAR" the memory of MATLAB between video files during
% the reviewing process, as not doing so will apply results loaded of the
% currently identified output.mat file to the previously reviewed video
% file and there will be mismatch (no red circles on identified objects).

```

```

% function viewOutputs

```

```

% Specify the file to be scanned:

```

```

% -----

```

```

% Modify these:

```

```

the_folder = 'C:\EXAMPLEFOLDER';

```

```

the_file = 'example_video.avi';

```

```

% Read the contents of the folder and identify the AVI-files:

```

```

[the_name] = strtok(the_file, '.');

```

```

output_file = strcat('output_',the_name, '.mat');

```

```

% Create a VideoReader object to connect to the file:

```

```

% -----

```

```

if ~exist('obj','var') || ~isa(obj,'VideoReader')

```

```

    obj = VideoReader(fullfile(the_folder,the_file));

```

```

end

```

```

% Load the results of the processing:

```

```

% -----

```

```

%v = load('output_'example_video.mat');

```

```

v = load(output_file);

```

```

% Find the frames in which bats were present:

```

```

% -----

```

```

idx = find(v.is_bat);

```

```

% Plot the analysis output data:

```

```

% -----
Figure(1)
plot(v.is_bat)
xlabel('Frame index')
ylabel('Potential target present')
pause

% Display multiple frames and show the bat locations:
% -----
%imageseq = 1:length(idx); % for all frames

for k = 1:length(idx) % Change first value (from "1") to start
% review further into clip
    % note that the number refers to nth idx
    Figure(idx(k)), clf % displays Figure using frame number
    showBats(obj, idx(k))
    pause
%     pause(0.03) % to pause the frames in seconds
    close(Figure(idx(k))) % to close the Figure
%     pause off
end

close(Figure(1)) % close frame index Figure

```

APPENDIX 2. OCCUPANCY MODEL COVARIATE STATISTICS

Descriptive statistics for occupancy (panel a) and detection probability covariates (panel b).

(a) Occupancy covariates

	precipitation (mm)	temperature (°C)	wind speed mean (m/s)	wind speed variability	wind speed max. (m/s)	wind direction (°)
Min.	0.00	18.06	1.61	0.72	2.27	1.45
1st Qu.	0.00	21.18	4.14	1.20	5.83	78.50
Median	1.06	22.34	5.73	1.48	8.38	88.60
Mean	7.66	22.11	5.55	1.57	8.12	111.93
SD	20.56	1.45	1.75	0.51	2.81	70.89
3rd Qu.	6.54	23.25	6.81	1.86	10.20	117.90
Max	199.60	25.09	10.33	4.48	15.17	358.47
NAs	0	0	0	0	0	0

(a) Occupancy covariates (continued)

	barometric pressure (mb)	relative humidity (%)	moon illumination (proportion)	Julian date (sine transformed)	Julian date (original)	Calendar date corresponding to Julian date
Min.	964.33	63.74	0.00	-1.0000	359	25-Dec
1st Qu.	970.40	79.36	0.17	-0.7056	313, 40	9-Nov, 9-Feb
Median	971.78	83.54	0.51	0.0000	268, 85	25-Sep, 26-Mar
Mean	971.65	83.60	0.51	0.0000	268, 85	25-Sep, 26-Mar
SD	1.95	5.93	0.35	0.7056	130, 222	10-May, 10-Aug
3rd Qu.	973.02	87.74	0.86	0.7056	130, 222	10-May, 10-Aug
Max	975.85	98.64	1.00	1.0000	176	25-Jun
NAs	0	27	0		0	

(b) Detection probability covariates

	canopy cover (%)	landcover heterogeneity (# types)	elevation (m)	terrain roughness (unitless)	topographic position (unitless)	wind exposure (m/s)
Min.	0	1	41	13.21	0.15	6.70
1st Qu.	0	2	162	22.19	0.47	7.38
Median	30	2	212	33.54	0.52	7.73
Mean	36.52	2.35	237	39.82	0.54	7.69
SD	35.80	0.89	121	22.74	0.18	0.61
3rd Qu.	69	3	370	49.55	0.66	8.00
Max	89	4	434	100.17	0.88	9.17
NAs	0	0	0	0	0	0

APPENDIX 3. PRELIMINARY SINGLE-COVIARIATE OCCUPANCY MODELS

Ranking of preliminary single-covariate models: (panel a) $\psi(\bullet)p(\text{cov})$, detection probability-only; (panel b) $\psi(\text{cov}) p(\bullet)$, occupancy-only. The notation (\bullet) indicates a constant parameter (i.e., modeled as an intercept only), and the null model includes no covariates and is shown as $\psi(\bullet)p(\bullet)$. Column AIC_c lists Akaike's information criterion values used to rank models based on best fit to the data, and column ΔAIC_c is the relative difference in values from the model with the smallest value. Column w is the model weight and column k is the number of model parameters. Only those parameters performing better than the null model were retained for future analyses

(a) Detection probability-only covariate models

Model parameter		AIC_c	ΔAIC_c	w	k
ψ	ρ				
•	canopy cover	2520.9	0.0	0.87	3
•	wind exposure	2524.7	3.7	0.13	3
•	topographic position	2558.7	37.7	0.00	3
•	landcover heterogeneity	2558.9	38.0	0.00	3
•	terrain roughness	2562.1	41.2	0.00	3
•	elevation	2569.5	48.6	0.00	3
•	•	2572.3	51.3	0.00	2

(b) Occupancy-only covariate models

Model parameter		AIC_c	ΔAIC_c	w	k
ψ	ρ				
relative humidity	•	2315.5	0.0	1.00	3
Julian date	•	2443.3	127.9	0.00	3
barometric pressure	•	2549.0	233.5	0.00	3
temperature	•	2549.8	234.4	0.00	3
wind direction	•	2563.0	247.6	0.00	4
wind speed variability	•	2571.0	255.5	0.00	3
precipitation	•	2571.9	256.4	0.00	3
•	•	2572.3	256.8	0.00	2
wind speed maximum	•	2572.3	256.8	0.00	3
wind speed mean	•	2572.8	257.3	0.00	3
moon illumination	•	2574.1	258.6	0.00	3

APPENDIX 4. FINAL OCCUPANCY MODELS

Ranking of final models used for model averaging. The null model includes no covariates and is shown as $\psi(\bullet)p(\bullet)$. Column AIC_c lists Akaike's information criterion values used to rank models based on best fit to the data, and column ΔAIC_c is the relative difference in values from the model with the smallest value. Column w is the model weight and column k is the number of model parameters.

Model parameter		AIC_c	ΔAIC_c	w	k
ψ	p				
Julian date + relative humidity + temperature + wind direction	canopy cover + elevation + topographic position + terrain roughness + wind exposure	2121.2	0.0	0.29	12
Julian date + barometric pressure + relative humidity + temperature + wind direction	canopy cover + elevation + topographic position + terrain roughness + wind exposure	2122.4	1.2	0.16	13
Julian date + relative humidity + temperature + wind direction	canopy cover + elevation + landcover heterogeneity + topographic position + terrain roughness + wind exposure	2123.0	1.8	0.12	13
Julian date + barometric pressure + relative humidity + temperature	canopy cover + elevation + topographic position + terrain roughness + wind exposure	2123.0	1.8	0.12	11
Julian date + relative humidity + temperature	canopy cover + elevation + topographic position + terrain roughness + wind exposure	2123.3	2.0	0.10	10
Julian date + barometric pressure + relative humidity + temperature + wind direction	canopy cover + elevation + landcover heterogeneity + topographic position + terrain roughness + wind exposure	2124.2	3.0	0.06	14
Julian date + barometric pressure + relative humidity + temperature	canopy cover + elevation + landcover heterogeneity + topographic position + terrain roughness + wind exposure	2124.8	3.6	0.05	12

Model parameter		AIC _c	ΔAIC _c	<i>w</i>	<i>k</i>
ψ	ρ				
Julian date + relative humidity + temperature	canopy cover + elevation + landcover heterogeneity + topographic position + terrain roughness + wind exposure	2125.0	3.8	0.04	11
Julian date + relative humidity + temperature + wind direction	canopy cover + elevation + landcover heterogeneity + topographic position + wind exposure	2126.0	4.7	0.03	12
Julian date + barometric pressure + relative humidity + temperature + wind direction	canopy cover + elevation + landcover heterogeneity + topographic position + wind exposure	2127.2	6.0	0.01	13
Julian date + barometric pressure + relative humidity + temperature	canopy cover + elevation + landcover heterogeneity + topographic position + wind exposure	2127.7	6.5	0.01	11
Julian date + relative humidity + temperature	canopy cover + elevation + landcover heterogeneity + topographic position + wind exposure	2127.9	6.7	0.01	10
•	•	2572.3	451.0	0.00	2

APPENDIX 5. FATALITY MODEL PARAMETERS

Evidence of absence modeling parameters for estimation of total fatalities. See Results section "Fatality Estimation" for description of parameters and values.

Parameter	Value
carcass count (m)	1
sampling coverage (A)	0.884
searcher efficiency mean (p)	0.850
lower 95% CI interval of p	0.760
upper 95% CI interval of p	0.920
proportion by which p changes with each search (k)	0.67
sampling interval (days)	1
sampling span (days)	182
persistence distribution	log-logistic
α (log-logistic scale)	1.64
mean β (log-logistic shape)	1.51
min β (log-logistic shape)	1.13
max β (log-logistic shape)	1.90
mean carcass persistence (CP)	3.07
estimated proportion of carcasses persisting through the interval (r)	0.850
prior distribution	uniform
max prior parameter	200
credibility level (1 - α)	0.900
arrival function	uniform